

AD-A007 947

ACOUSTIC FATIGUE DESIGN DATA. PART IV

ADVISORY GROUP FOR AEROSPACE RESEARCH AND
DEVELOPMENT

JANUARY 1975

DISTRIBUTED BY:

NTIS

National Technical Information Service
U. S. DEPARTMENT OF COMMERCE

AD. A 007 947

REPORT DOCUMENTATION PAGE			
1. Recipient's Reference	2. Originator's Reference	3. Further Reference	4. Security Classification of Document
	AGARD-AG-162		UNCLASSIFIED
5. Originator	Advisory Group for Aerospace Research and Development North Atlantic Treaty Organization 7 rue Ancelle, 92200 Neuilly sur Seine, France		
6. Title	Acoustic Fatigue Design Data		
7. Presented at			
8. Author(s)	A.G.R.Thomson and R.F.Lambert		9. Date
			January 1975
10. Author's Address	Engineering Sciences Data Unit Ltd. 251-259 Regent Street, London W1R 7AD		11. Pages
			46
12. Distribution Statement	This document is distributed in accordance with AGARD policies and regulations, which are outlined on the Outside Back Covers of all AGARD publications.		
13. Keywords/Descriptors	Fatigue (materials) Box beams Acoustics Resonant frequency Tests Loads (forces)		14. UDC
			539.433:620.178.3: 629.73.023.4
15. Abstract	<p>This is the fourth and final portion of this AGARDograph on Acoustic Fatigue Design Data. It contains acoustic fatigue test procedures, methods of calculation and results for various structural elements. Section I presents a method to determine the natural frequencies of initially unstressed box structures that are rectangular in section. The second section provides a method of estimating the R.M.S. stress in internal plates of a box structure subjected to random acoustic loading. Section III provides a method of estimating the sound pressure levels within the intake duct of a supersonic fan or compressor due to buzz saw noise.</p> <p>This AGARDograph was sponsored by the Structures and Materials Panel of AGARD.</p>		

Reproduced by
NATIONAL TECHNICAL
INFORMATION SERVICE
US Department of Commerce
Springfield, VA 22151

PRICES SUBJECT TO CHANGE

NORTH ATLANTIC TREATY ORGANIZATION
ADVISORY GROUP FOR AEROSPACE RESEARCH AND DEVELOPMENT
(ORGANISATION DU TRAITE DE L'ATLANTIQUE NORD)

AGARDograph No.162
ACOUSTIC FATIGUE DESIGN DATA
Part IV

by

A.G.R.Thomson and R.F.Lambert
Engineering Sciences Data Unit Ltd
London, UK

THE MISSION OF AGARD

The mission of AGARD is to bring together the leading personalities of the NATO nations in the fields of science and technology relating to aerospace for the following purposes:

- Exchanging of scientific and technical information;
- Continuously stimulating advances in the aerospace sciences relevant to strengthening the common defence posture;
- Improving the co-operation among member nations in aerospace research and development;
- Providing scientific and technical advice and assistance to the North Atlantic Military Committee in the field of aerospace research and development;
- Rendering scientific and technical assistance, as requested, to other NATO bodies and to member nations in connection with research and development problems in the aerospace field;
- Providing assistance to member nations for the purpose of increasing their scientific and technical potential;
- Recommending effective ways for the member nations to use their research and development capabilities for the common benefit of the NATO community.

The highest authority within AGARD is the National Delegates Board consisting of officially appointed senior representatives from each member nation. The mission of AGARD is carried out through the Panels which are composed of experts appointed by the National Delegates, the Consultant and Exchange Program and the Aerospace Applications Studies Program. The results of AGARD work are reported to the member nations and the NATO Authorities through the AGARD series of publications of which this is one.

Participation in AGARD activities is by invitation only and is normally limited to citizens of the NATO nations.

The content of this publication has been reproduced directly from material supplied by AGARD or the authors.

Published January 1975

Copyright © AGARD 1975

539.433:620.178.3:629.73.023.4

National Technical Information Service is authorized to reproduce and sell this report.



*Printed by Technical Editing and Reproduction Ltd
Harford House, 7-9 Charlotte St, London, W1P 1HD*

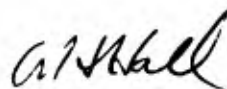
PREFACE

This volume, the fourth and final part of a series giving data for design against acoustic fatigue, has been prepared in order to draw together the results of research in acoustic fatigue and to present them in a form directly useable in aerospace design.

The AGARD Structures and Materials Panel has for many years been active in encouraging and coordinating the work that has been necessary to make this collection of design data possible and after agreeing on procedures for the acquisition, analysis and interpretation of the requisite data, work on this series of design data sheets was initiated in 1970.

The overall management of the project has been conducted by the Working Group on Acoustic Fatigue of the AGARD Structures and Materials Panel, and the project has been financed through a collective fund established by the Nations collaborating in the project, namely Canada, France, Germany, Italy, UK and US. National Coordinators appointed by each country have provided the basic data, liaised with the sources of the data, and provided constructive comment on draft data sheets. These Coordinators are Dr G.M. Lindberg (Canada), Mr R. Loubet (France), Mr G. Bayerdörfer (Germany), Gen. A. Griselli (Italy), Mr N.A. Townsend (UK), Mr A.W. Kolb (US) and Mr F.F. Rudder (US). Staff of the Engineering Sciences Data Unit Ltd London, have analysed the basic data and prepared and edited the resultant data sheets with invaluable guidance and advice from the National Coordinators and from the Acoustic Fatigue Panel of the Royal Aeronautical Society which has the following constitution: Professor B.L. Clarkson (Chairman), Mr D.C.G. Eaton, Mr J.A. Hay, Mr W.T. Kirkby, Mr M.J.T. Smith and Mr N.A. Townsend. The members of staff of the Engineering Sciences Data Unit concerned with the preparation of the data sheets in this volume were: Mr A.G.R. Thomson (Executive, Environmental Projects), Mr R.F. Lambert (Environmental Projects Group) and Mrs A.R. Green (Environmental Projects Group).

Data sheets based on this AGARDograph will subsequently be issued in the Fatigue Series of Engineering Sciences Data issued by ESDU Ltd. where additions and amendments will be made to maintain their current applicability.



A.H. Hall
Chairman,
Working Group on Acoustic Fatigue
Structures and Materials Panel

CONTENTS

		<u>Page No.</u>
SECTION 1.	NATURAL FREQUENCIES OF BOX STRUCTURES	
	1.1 Notation	1
	1.2 Introduction	2
	1.3 Notes	2
	1.4 Comparison with Measured Data	3
	1.5 Derivation and Reference	4
	1.6 Example	4
	Figures	6
	APPENDIX	
	1A Computer Program	15
SECTION 2.	ESTIMATION OF R.M.S. STRESS IN INTERNAL PLATES OF A BOX STRUCTURE SUBJECTED TO RANDOM ACOUSTIC LOADING	
	2.1 Notation	18
	2.2 Introduction	18
	2.3 Notes	19
	2.4 Calculation Procedure	19
	2.5 Comparison with Measured Data	20
	2.6 Derivation and References	21
	2.7 Example	21
	Figures	21
		23
SECTION 3.	ESTIMATION OF SOUND PRESSURE LEVELS DUE TO BUZZ-SAW NOISE WITHIN THE INTAKE DUCT OF A SUPERSONIC FAN OR COMPRESSOR	
	3.1 Introduction	29
	3.2 Notation	29
	3.3 Notes	29
	3.4 Derivation	31
	3.5 Example	31
	Figures	31
		34

Section 1

NATURAL FREQUENCIES OF BOX STRUCTURES

1.1 Notation

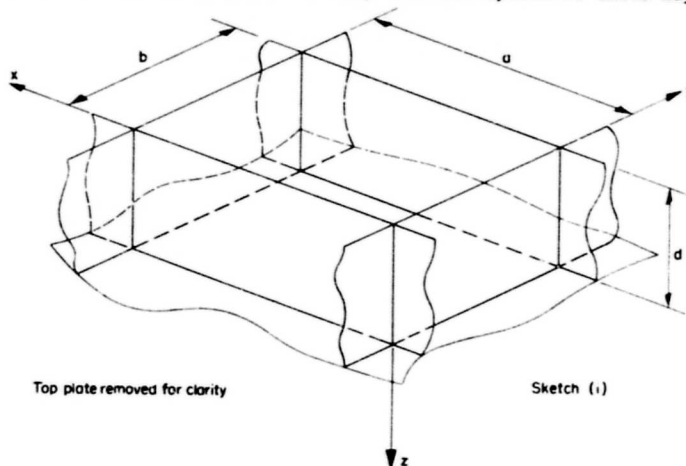
a	length of longer side of skin plate	m	in
b	length of shorter side of skin plate	m	in
d	depth of box	m	in
E	Young's modulus	N/m ²	lbf/in ²
f	natural frequency	Hz	c/s
K	frequency parameter	m/s	in/s
m	mode number in x-direction		
n	mode number in y-direction		
q	mode number in z-direction		
t	plate thickness	m	in
V	velocity parameter for plate material*		
x,y,z	rectangular system of Cartesian coordinates defined in Sketch (1)		
ρ	density of plate material	kg/m ³	+
σ	Poisson's ratio of plate material		

Suffixes

c	cover plate in xy- plane (e.g. skin)
r	internal plate in xz- plane (e.g. rib)
s	internal plate in yz- plane (e.g. spar web or frame)

It is conventional, in aircraft engineering, to refer to plates of a box structure as skins, ribs and spars as above. This nomenclature is used in this data sheet for convenience.

Both SI and British units are quoted but any coherent system of units may be used.



Top plate removed for clarity

Sketch (1)

* The velocity parameter is defined in SI units by $V = (E/\rho)^{1/2}/5080$ or in British units by $V = (E/\rho)^{1/2}/200\,000$. It is approximately unity for all common structural metallic materials.

+ A density value expressed in British units as pounds per cubic inch has to be divided by 386.4 before being used to calculate parameters defined in this Section. (A force of 1 lbf acting on a mass of 1 lb produces an acceleration of 386.4 in/s².)

1.2 Introduction

Many aircraft have structures of box form in regions of dynamic loading. This loading may be due to jet noise, boundary layer noise, buffet or other types of loading action. This data sheet is primarily intended for use with box structures excited by jet noise but is applicable to other types of dynamic loading.

Examples of box structures are typically found in jet aircraft in fin and tailplane structures. In jet aircraft, in the usual configurations, these structures lie close to the jet efflux, a region of intense acoustic loading. Fin and tailplane structures are usually built-up from pairs of skin panels separated by ribs and spar webs. In terms of dynamic response the ribs and spars provide a mechanical coupling between opposite skin plates. Practical structures have cut-outs in ribs and spars which increase the complexity of the analysis and thereby make exact solution beyond the scope of a data sheet presentation. However, a simple idealised structure leads to a qualitative understanding of the major response characteristics.

In the simple analysis presented in this Section, it is implicit that the vibrations of the skin and internal supporting structure are coupled. In practice it is unlikely that skin and internal plates are completely coupled in any mode of vibration. The nature of the response is dependent on both the nature of the exciting noise field and structural relationships.

To assess the effectiveness of a noise source in exciting a particular mode of vibration, the exciting force phase relationship over the structure must be considered. When the exciting force varies in a random manner, as does jet noise, the phase relationships will not be constant with time. In such cases it is usual to consider the pressure correlation which indicates the average phase relationship between pressures at two points over a period of time. Tests on jet aircraft structures have shown that, within the frequency range of interest for typical structures, the pressure correlation is likely to be high and positive (pressure in-phase) over a number of skin panels. This tends to favour the vibration modes where adjacent skin panels are in-phase and there is relatively little distortion of ribs (or spars), rather than the modes which occur when skin and rib plates are coupled so that adjacent skin panels are out of phase and there is considerable rib distortion.

For skin and rib vibrations to be coupled, such that the plates vibrate together with one frequency and with comparable amplitudes, their stiffnesses and mass distribution must be closely related. Representing a symmetric box, with equal top and bottom skin thickness, by a simple two-dimensional beam model suggests that when the individual skin and rib frequencies are equal the box fundamental mode is one in which skin and rib plates vibrate together in a simply-supported type of mode. This condition occurs when $(d/b)(t_c/t_r)^{1/2}$ is unity. In box structures where rib stiffness is greater than skin stiffness, the lowest frequency mode is that in which individual skin plates vibrate in their fixed-edge mode.

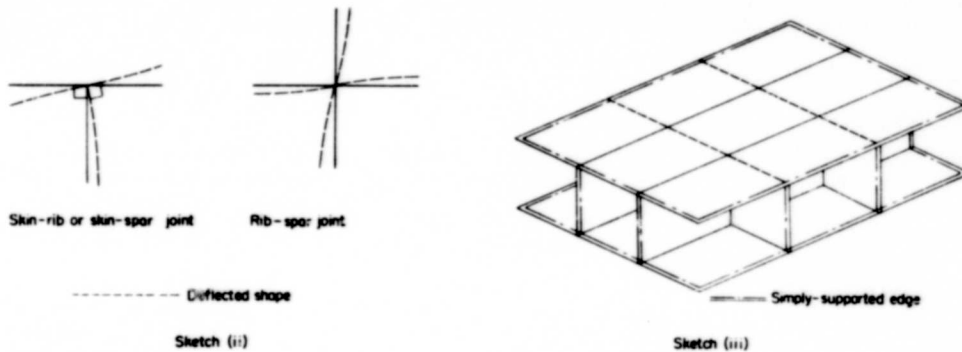
Coupled plate vibrations are less likely to occur in box arrays with non-uniformities since they induce a decoupling effect. Likely non-uniformities are unequal rib pitches or differences between stiffnesses of the top and bottom skin-stiffener combinations.

It is evident from the preceding discussion that fully coupled skin and rib vibration modes occur only in certain conditions of the noise field and structure geometry. If, when estimating frequencies of vibration as a first step towards the calculation of fatigue life in an acoustic environment, the coupled mode conditions are not satisfied it is better to consider the individual elements (skin plates and rib plates) separately. Estimates of plate natural frequencies may be obtained from Part I, Sections 3 or 4 or Part II, Section 2 of this AGARDograph.

1.3 Notes

This Section gives the natural frequencies of box structures that are rectangular in section and initially unstressed. The data presented are based on the theory given in Derivation 1.5.4 where a Rayleigh analysis, which uses an assumed sinusoidal mode shape, is applied to a nine-cell box structure. The theoretical analysis allows for rotation at plate joints but the joints are fixed against translation. All angles at the joints between skin and ribs, or spars, are assumed to remain at

90° throughout the vibratory motion. Within the limits of the simple analysis it is impossible to apply the 90° joint restraint to rib-to-spar joints (see Sketch (ii)); however, this joint is considered to be the least important for the frequency calculation. All exterior edges of the nine-cell box structure are assumed to be simply-supported (see Sketch (iii)).



The graphical presentation of data is restricted to the lowest natural frequency (i.e. $n = m = q = 1$) for a box within an array of identical boxes having equal upper and lower skin thicknesses. The deflected shape of this mode, through the centre of the box, in both the xz -plane and yz -plane is shown in Sketch (iv). The computer program, in Appendix 1A, can be used to obtain frequencies of higher modes as well as those for boxes in an array having skin plates of any aspect ratio and with any or all of the plates of different thickness.

The lowest natural frequency is intended for use in calculating the stress response of box structure panels under the action of acoustic loading. This frequency is given by

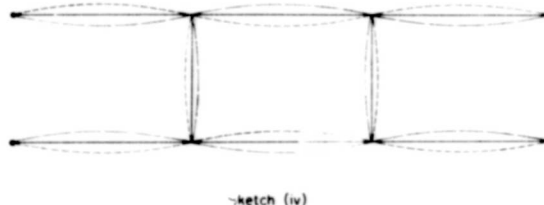
$$f = VK \frac{t_c}{b^2}$$

In Figures 1.1 - 1.8, values of K are presented as carpets in terms of the plate parameters b/a and b/d . Carpets are given for a range of values of t_c/t_r for each of four values of t_s/t_c .

In deriving the curves, the value of σ was assumed to be 0.3. This value gives sufficiently accurate frequencies for all common structural metallic materials. The mode number is taken to be the number of half waves in the relevant plate direction.

This data sheet provides a means of assessing the effects that changes in geometric parameter have on frequency; however, the predicted frequencies can be only approximate because of the assumptions made in the analysis. A comparison of estimated and measured frequencies is provided (see paragraph 1.4).

This Section may be used to obtain a first approximation to the natural frequencies of box structures having skins with stiffeners between the ribs, or frames. In this case an equivalent skin thickness should be used. It is recommended that this equivalent skin thickness should be that necessary to give the same frequency as that of the stiffened plate. The equivalent skin thickness is dependent on the mode of vibration of the stiffened plate. For a stiffened plate vibrating in a fundamental type mode, the frequency may be obtained from Part I, Section 3 (conventionally stiffened panel) or Part III, Section 3 (integrally machined panel) of this AGARDograph; then using Reference 1.5.7 the thickness of the flat, unstiffened panel of the same aspect ratio and having the stiffened panel natural frequency can be obtained. The calculation and use of effective skin thickness in estimating the frequency for a box with stiffened skin is shown in the example in Paragraph 1.6.2.



1.4 Comparison with Measured Data

Figure 1.9 shows a comparison of calculated natural frequencies and measured frequencies of rectangular box structures. All boxes considered are idealised structures, i.e. without cut-outs or stiffeners between ribs or spars. Some of these data are from structures excited by random acoustic loading where the modes of vibration were not identified. In such cases the measured frequency of the maximum root mean square strain has been compared with the calculated lowest natural frequency.

The fundamental vibratory mode of a plate is the mode most sensitive to edge support conditions. As the deflected shape used in the analysis assumes simply-supported edges the predicted frequency for the (0,1) mode is generally lower than the measured value.

1.5 Derivation and Reference

Derivation

- 1.5.1 Clarkson, B.L.
Ford, R.D. The response of a typical aircraft structure to jet noise. J.R. aeronaut.Soc., Vol. 66, No.613, pp. 31-40, January 1962.
- 1.5.2 Clarkson, B.L. The design of structures to resist jet noise fatigue. J.R. aeronaut.Soc., Vol. 66, No.622, pp. 603-616, October 1962.
- 1.5.3 Barrett, G.W. Fatigue and response testing of riveted joints in panels subjected to wide band loading in the B.A.C. (Weybridge) high intensity noise facility. British Aircraft Corporation Ltd, Acoustics Lab. Rep. No.048 Part 2. Work under Ministry of Technology Contract KS/1/0504/CB.43A2, November 1970.
- 1.5.4 Rudder, F.F. Acoustic fatigue of aircraft structural component assemblies. Air Force Flight Dynamics Lab., Ohio, tech.Rep. AFFDL-TR-71-107, February 1972.
- 1.5.5 Abrahamson, A.L. Structural response to aero-acoustic noise. British Aircraft Corporation Ltd, Acoustics Lab. Rep. No.364. Work under Ministry of Technology, Contract KS/1/0632/CB.43A2, 1973.
- 1.5.6 Clarkson, B.L. Estimates of the response of box type structures to acoustic loading. Paper 10 of Proceedings of symposium on acoustic fatigue, Toulouse, September 1972. AGARD-CP-113, May 1973.

Reference

- 1.5.7 - Natural frequencies of uniform flat plates. Engineering Sciences Data Item No.66019, February 1966.

1.6 Example

1.6.1

It is required to estimate the lowest natural frequency of an aluminium alloy box structure made up from identical cells having top and bottom skin plates of equal thickness, with the following dimensions and physical properties:

$$\begin{aligned} a &= 600 \text{ mm}, & b &= 200 \text{ mm}, & d &= 150 \text{ mm}, \\ t_c &= 0.8 \text{ mm}, & t_r &= 0.8 \text{ mm}, & t_b &= 1.2 \text{ mm}, \\ E &= 70\,000 \text{ MN/m}^2, & \rho &= 2770 \text{ kg/m}^3, & \sigma &= 0.3. \end{aligned}$$

Firstly

$$\frac{b}{a} = \frac{200}{600} = 0.33,$$

$$\frac{b}{d} = \frac{200}{150} = 1.33,$$

$$\frac{t_c}{t_r} = \frac{0.8}{0.8} = 1.0,$$

and $\frac{t_b}{t_c} = \frac{1.2}{0.8} = 1.5.$

From Figure 1.4 $K = 3.0 \times 10^3 \text{ m/s}$ for $\frac{t_b}{t_c} = 1.0,$

and from Figure 1.6 $K = 3.22 \times 10^3 \text{ m/s}$ for $\frac{t_b}{t_c} = 2.0.$

By linear interpolation for $\frac{t_b}{t_c} = 1.5, K = 3.11 \times 10^3 \text{ m/s}.$

$$\text{Also } V = \sqrt{\frac{70\,000 \times 10^6}{2770}} \times \frac{1}{5080} = 0.99.$$

$$\begin{aligned} \text{Hence } f &= 0.99 \times 3.11 \times 10^3 \times \frac{0.8 \times 10^{-3}}{(200 \times 10^{-3})^2} \\ &= 61.6 \text{ Hz.} \end{aligned}$$

The example illustrates that within the limits of accuracy of the frequency prediction, the calculation of V is unnecessary for boxes constructed from metals commonly used in structures; its value may be assumed to be 1.0.

1.6.2

If conventional Z-section stringers are riveted to the top and bottom skin plates parallel to the box sides of length 200 mm, at a uniform pitch of 150 mm, find the new box frequency using an effective skin thickness.

The stringer geometric and physical properties are as follows:

St Venant constant of uniform torsion, J_{st} , equals $11.7 \times 10^{-2} \text{ m}^4$,

polar moment of inertia of the stringer cross section about a point on the skin directly beneath the stringer shear centre, I_{st} , equals $11.0 \times 10^{-9} \text{ m}^4$,

warping constant of the stringer cross section with respect to the point on the skin directly beneath the stringer shear centre, Γ_{st} , equals $4.93 \times 10^{-13} \text{ m}^6$.

Young's modulus, $E_{st} = 70\,000 \text{ MN/m}^2$,

shear modulus, $G_{st} = 27\,000 \text{ MN/m}^2$

and density $\rho_{st} = 2770 \text{ kg/m}^3$.

The flexural rigidity per unit width of the skin plate is given by

$$\begin{aligned} \frac{Et_c^3}{12(1-\sigma^2)} &= \frac{70\,000 \times 10^6 \times (0.8 \times 10^{-3})^3}{12(1-0.3^2)} \\ &= 3.28 \text{ N m.} \end{aligned}$$

Using the above values in Part I, Section 3 of this AGARDograph the lowest natural frequency is found to be 212 Hz.

From Part I, Section 4 of this AGARDograph (or Reference 1.5.7) the fundamental natural frequency parameter for the flat, unstiffened panel of aspect ratio $\frac{200}{150} = 1.33$ is $3.78 \times 10^3 \text{ m/s}$.

Therefore, if t_{ce} is the effective plate thickness,

$$3.78 \times 10^3 \times \frac{t_{ce}}{0.15^2} = 212$$

which gives $t_{ce} = 1.26 \text{ mm}$.

$$\text{Then } \frac{t_{ce}}{t_r} = \frac{1.26}{0.8} = 1.58,$$

$$\text{and } \frac{t_s}{t_{ce}} = \frac{1.2}{1.26} = 0.95.$$

From Figure 1.4 $K = 3.02 \times 10^3 \text{ m/s}$ for $\frac{t_c}{t_r} = 1.0$

and $K = 2.70 \times 10^3 \text{ m/s}$ for $\frac{t_c}{t_r} = 2.0$

By linear interpolation for $\frac{t_c}{t_r} = 1.58$, $K = 2.83 \times 10^3 \text{ m/s}$.

Hence frequency for the box with stiffened skin plates

$$\begin{aligned} &= 0.99 \times 2.83 \times 10^3 \times \frac{1.26 \times 10^{-3}}{(200 \times 10^{-3})^2} \\ &= 88.3 \text{ Hz.} \end{aligned}$$

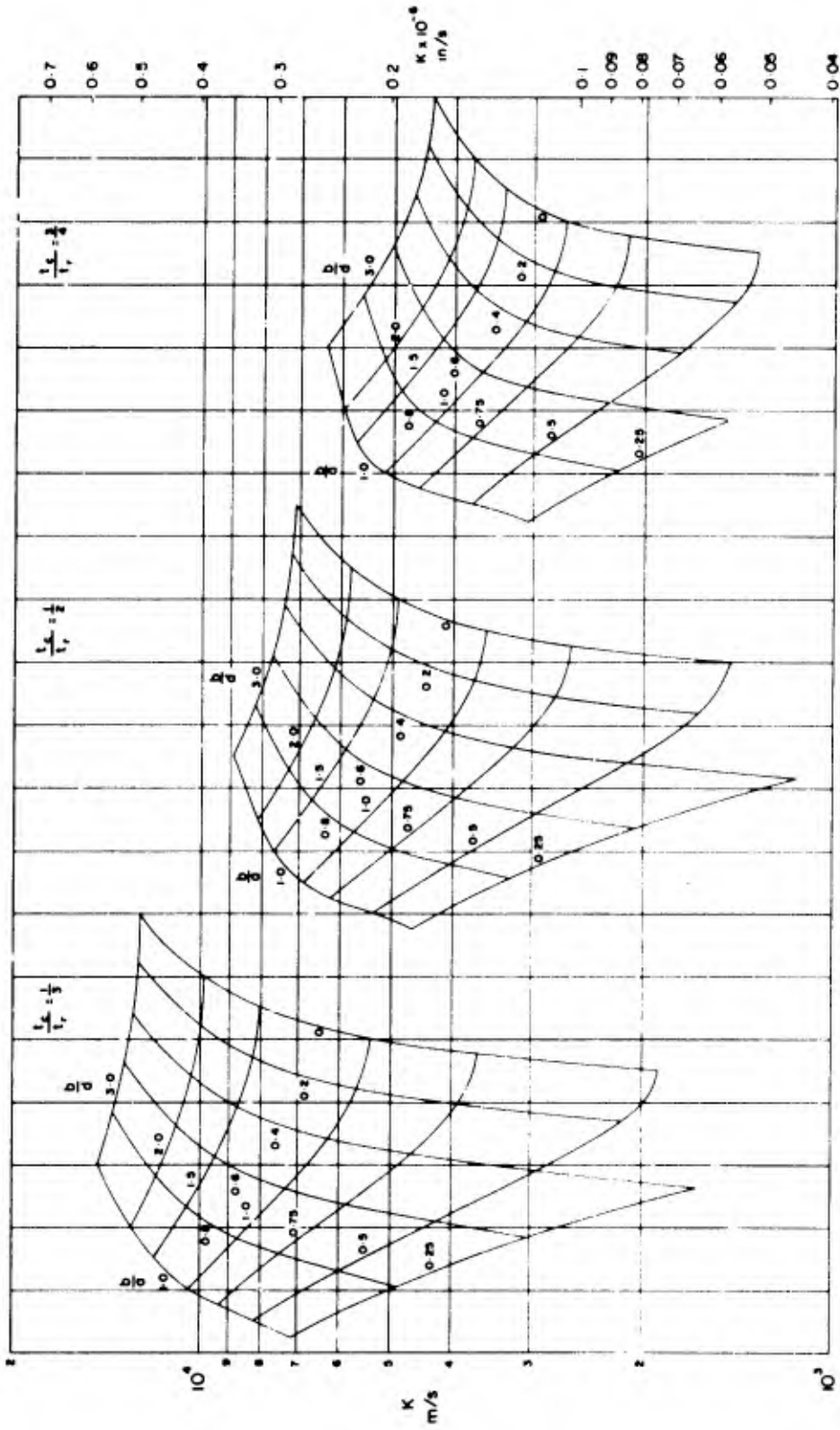


FIGURE 11 FREQUENCY PARAMETER FOR $\frac{1}{2} \frac{\lambda}{l} = 0.5$

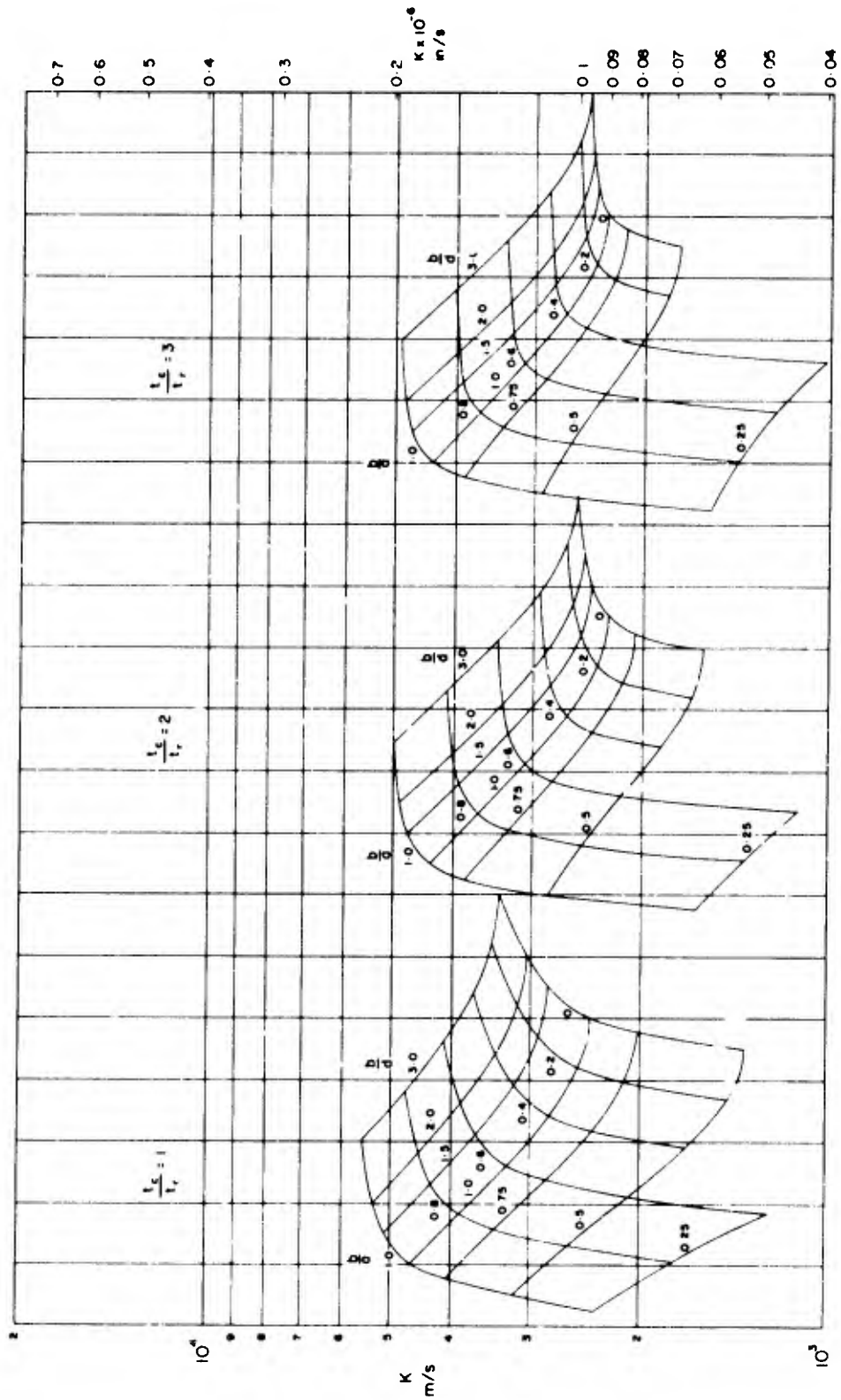


FIGURE 1.2 FREQUENCY PARAMETER FOR $\frac{l_2}{l_1} = 0.5$

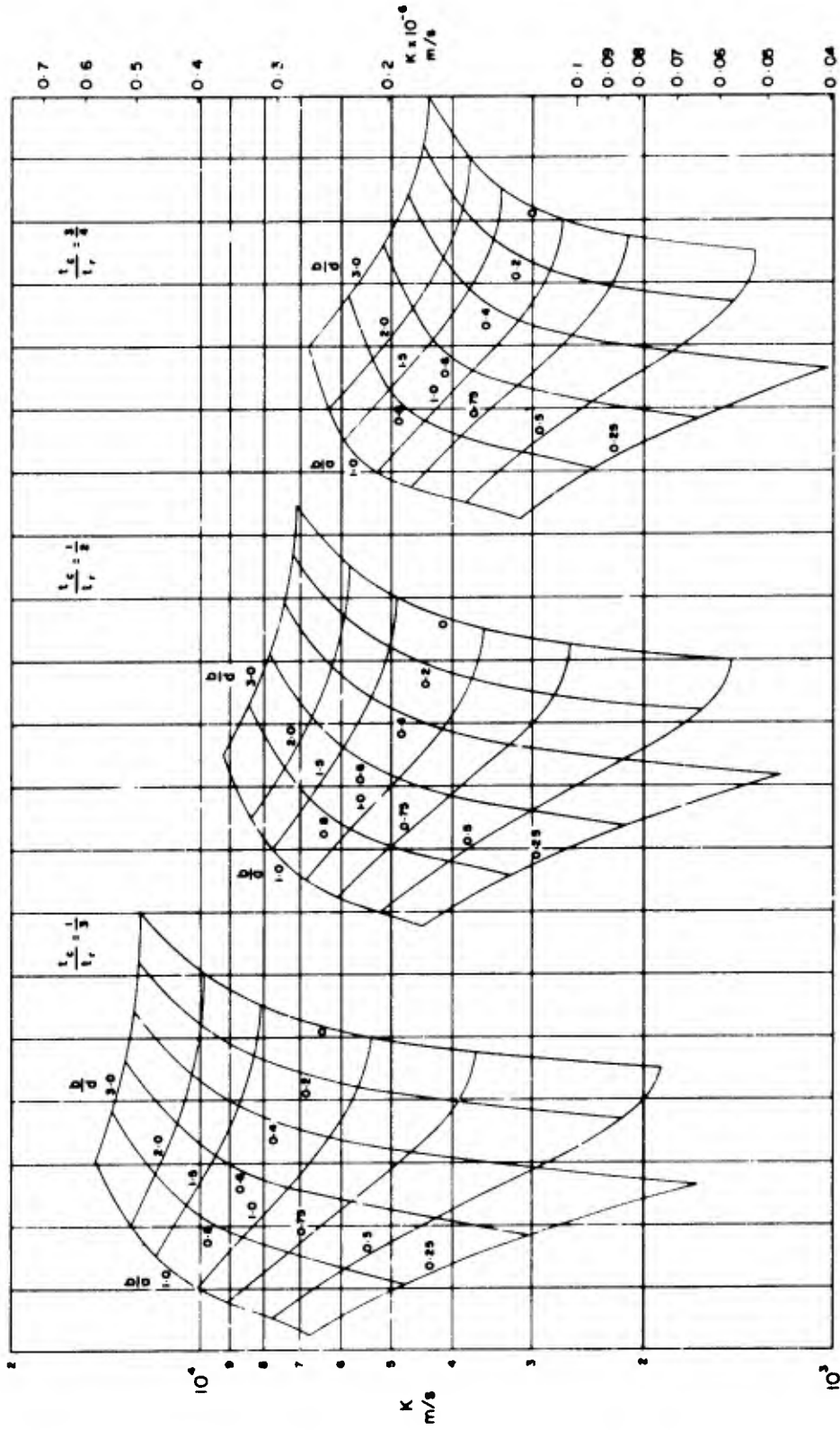


FIGURE 1.3 FREQUENCY PARAMETER FOR $\frac{l_2}{l_1} = 1.0$

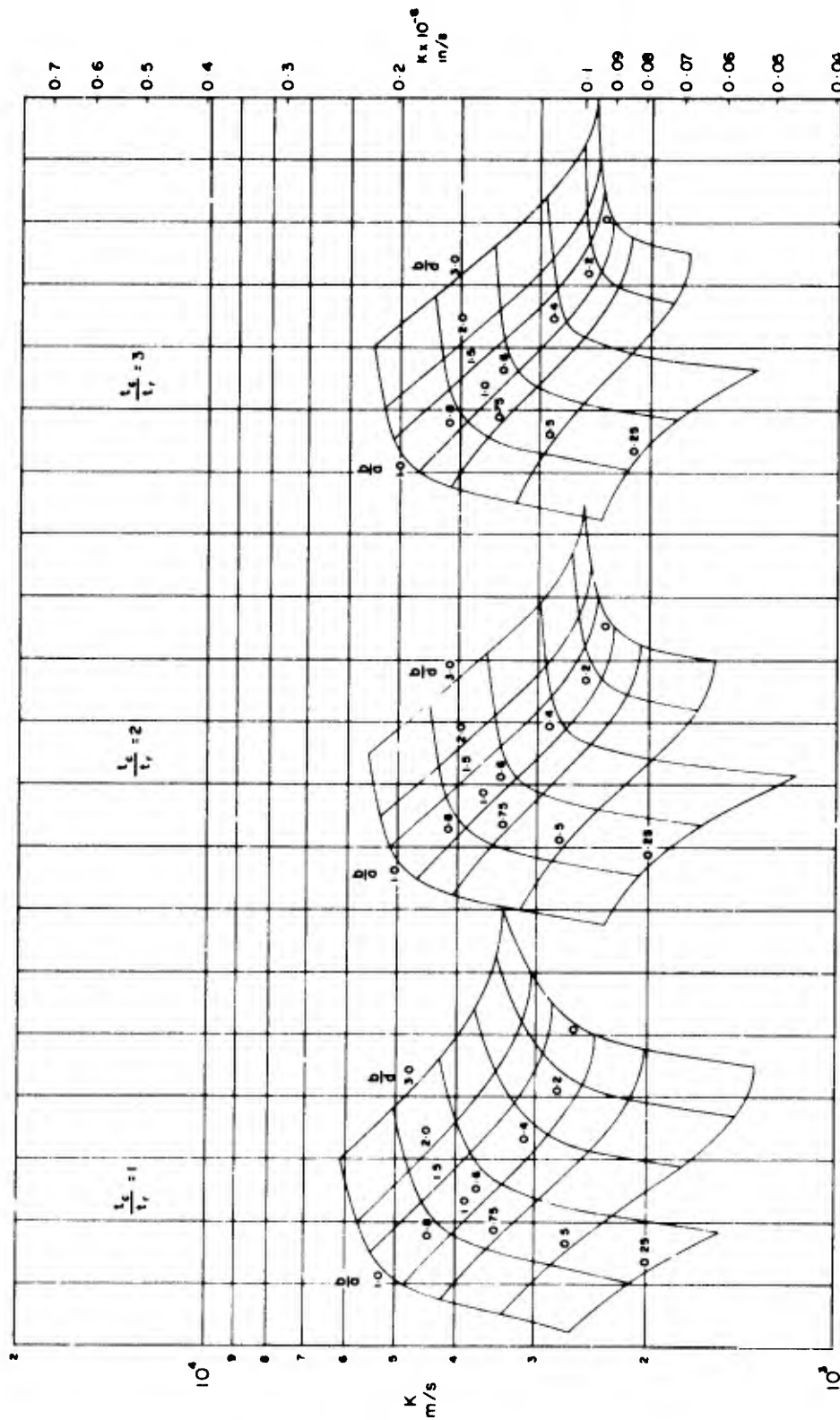


FIGURE 1.4 FREQUENCY PARAMETER FOR $\frac{l_2}{l_1} = 1.0$

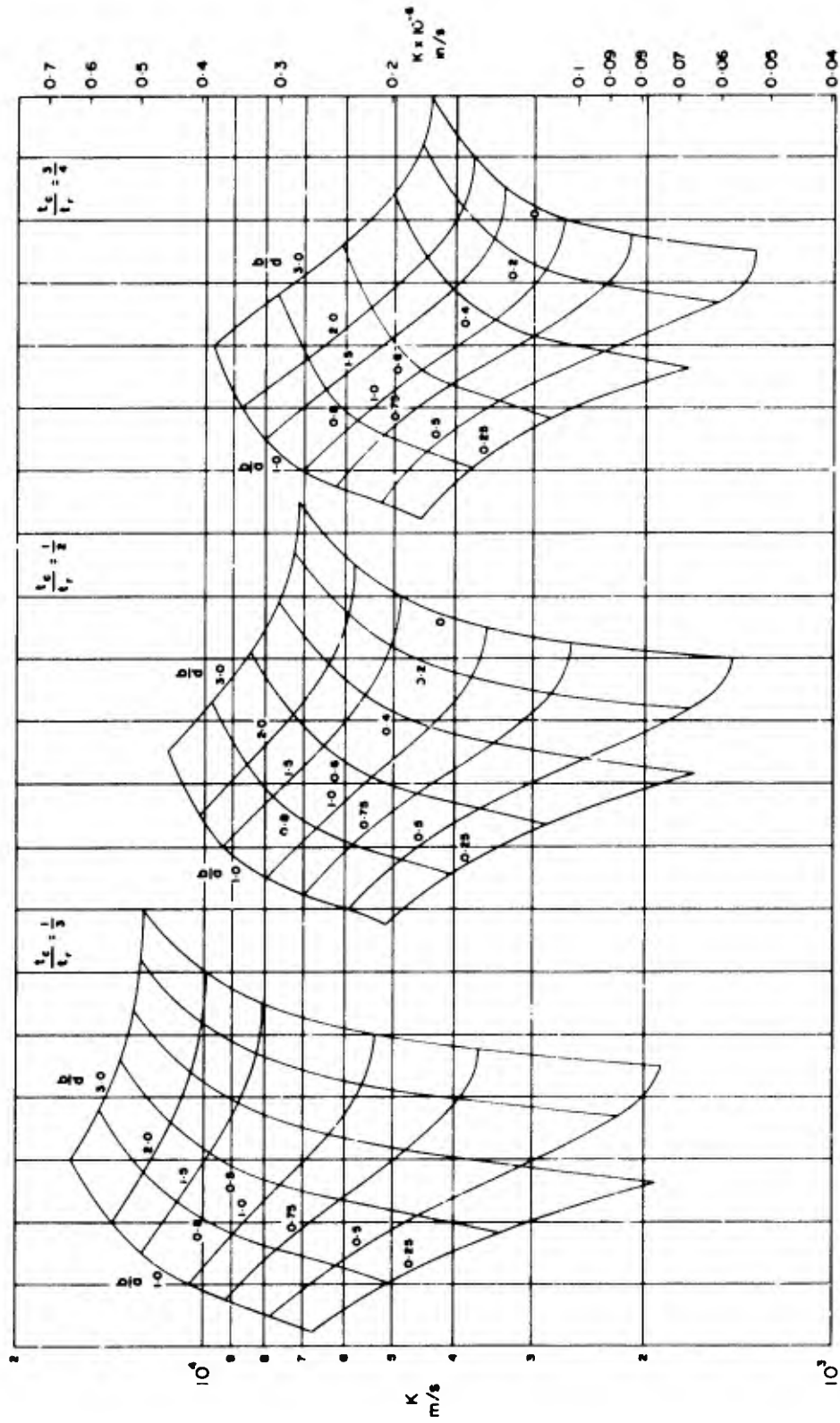


FIGURE 1.5 FREQUENCY PARAMETER FOR $\frac{t_c}{t_c} = 2.0$

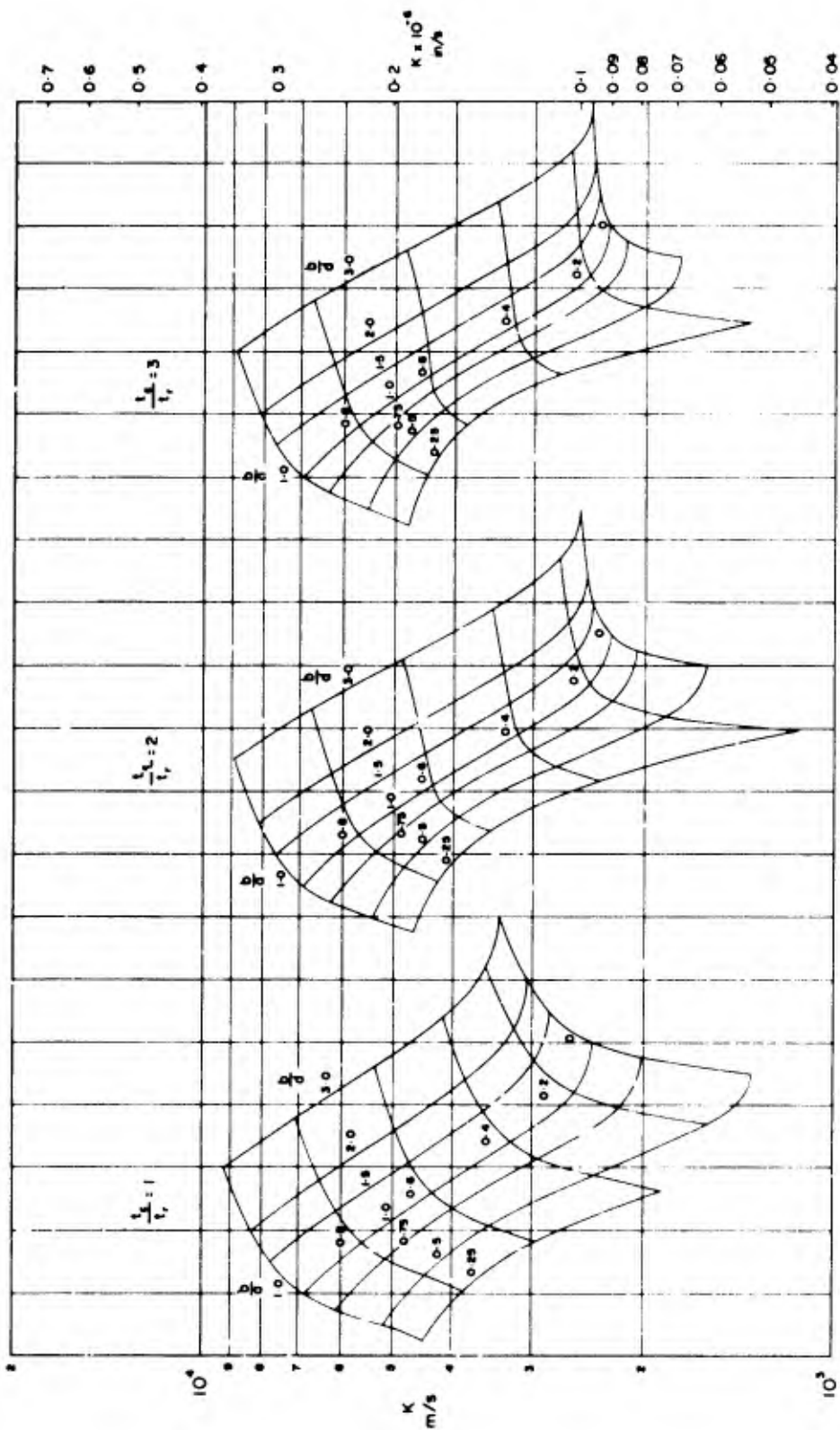


FIGURE 16 FREQUENCY PARAMETER FOR $\frac{t_c}{t_s} = 2$ 0

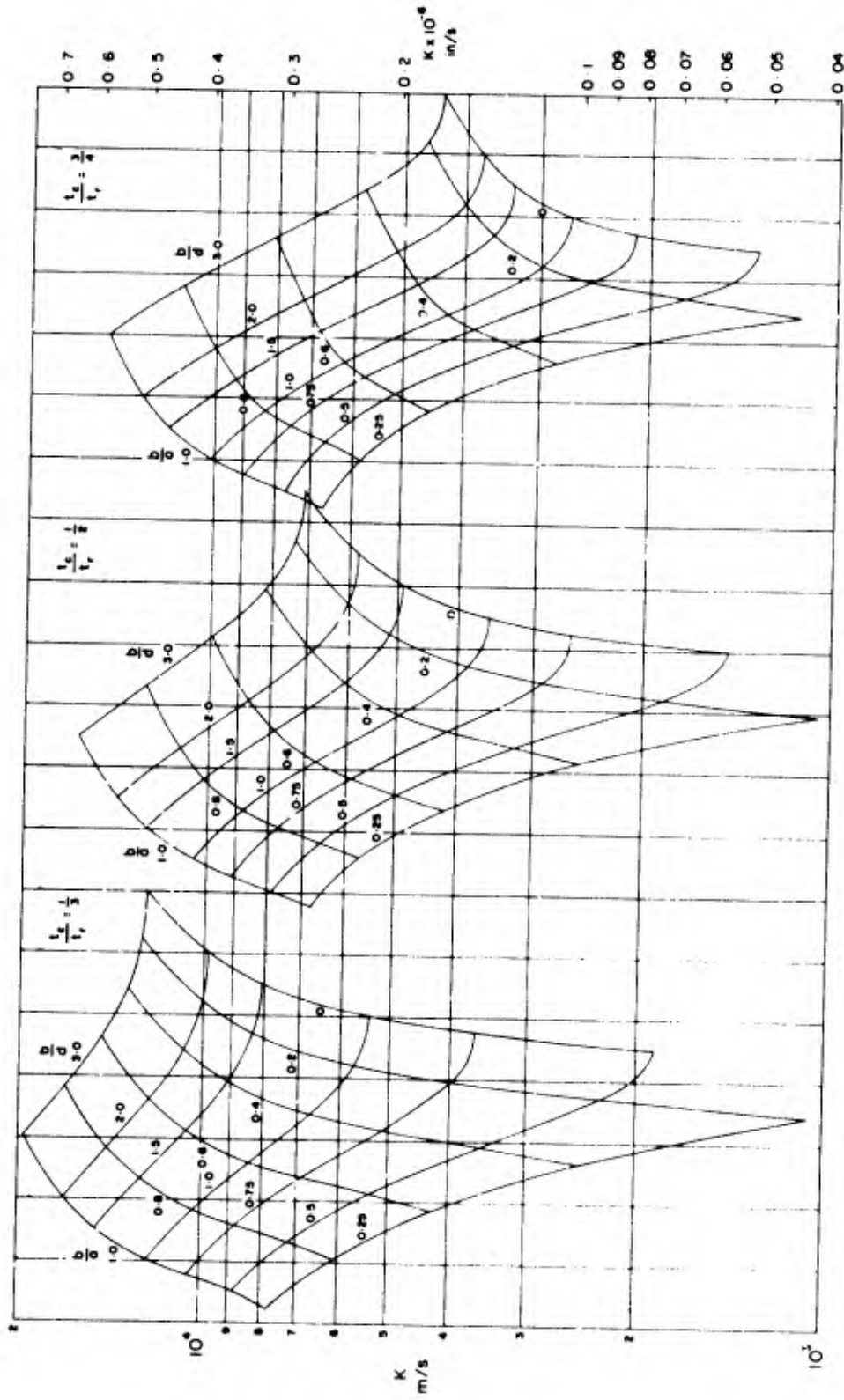


FIGURE 17 FREQUENCY PARAMETER FOR $\frac{L_2}{L_1} = 3.0$

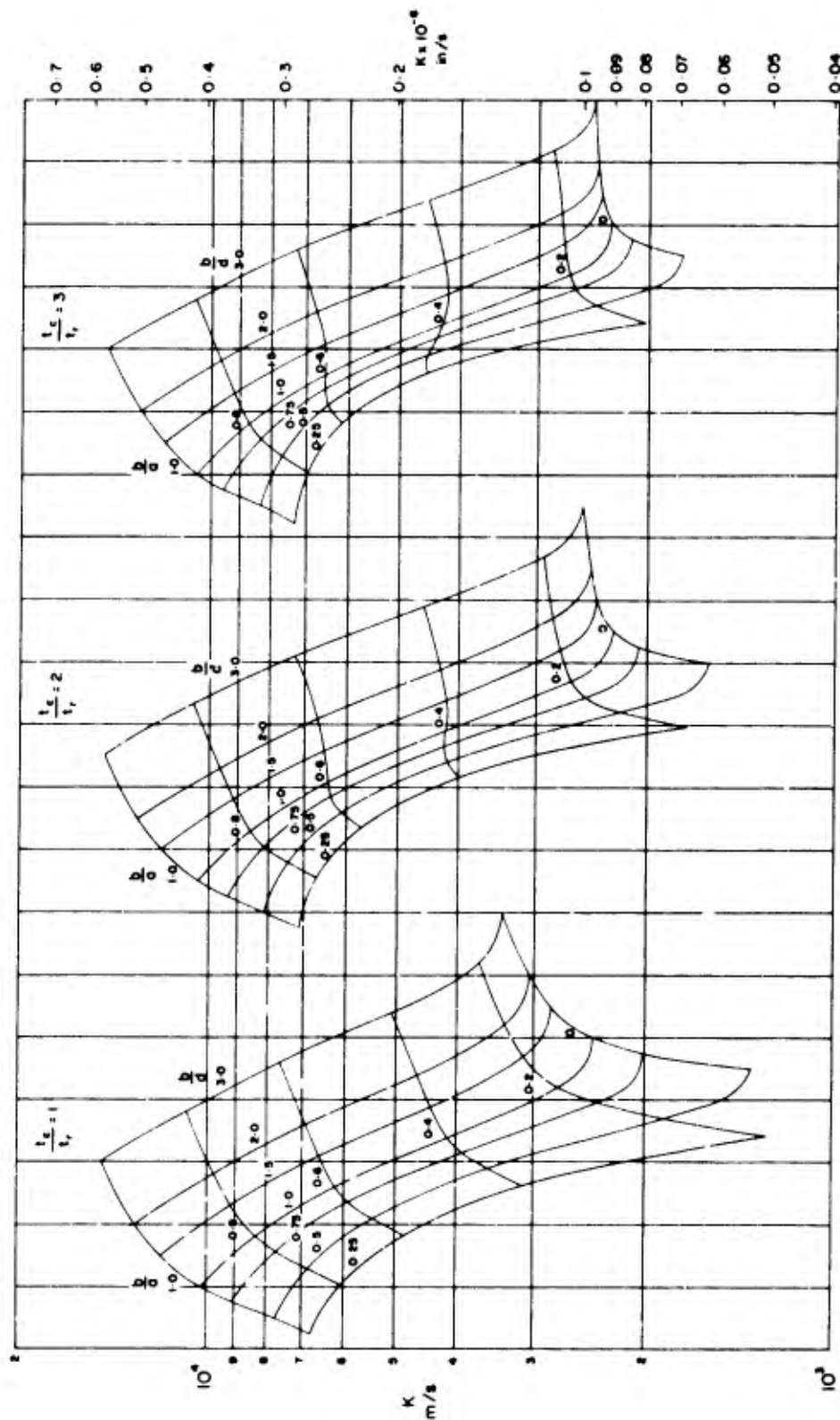


FIGURE 1.8 FREQUENCY PARAMETER FOR $\frac{t_2}{t_1} = 3.0$

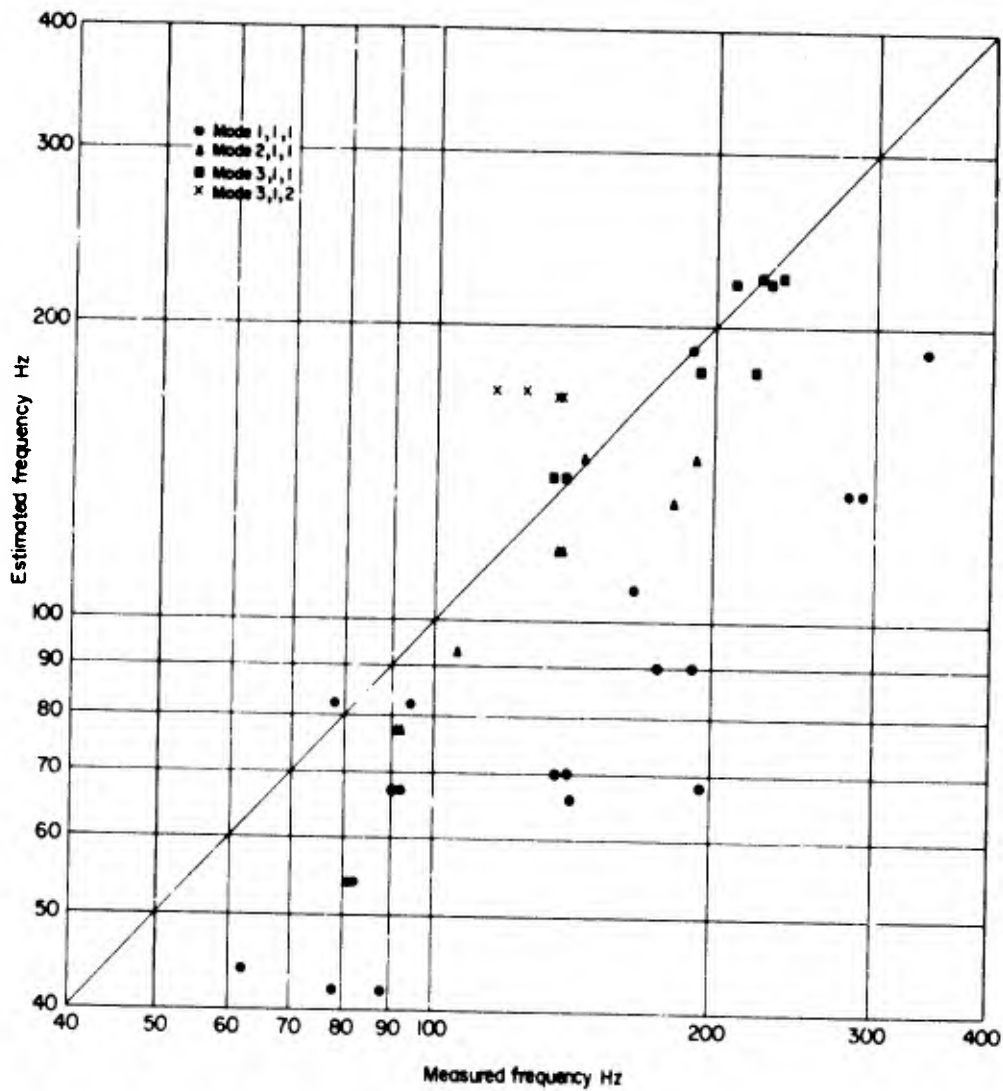


FIGURE 19 COMPARISON OF ESTIMATED AND MEASURED NATURAL FREQUENCIES

Appendix IAComputer ProgramIA.1 General Notes

The natural frequencies of a box structure, made up from rectangular cells, may be found using this computer program. The assumptions given in paragraph 1.3 are applicable to this program as are the requirements for coupling of cover plate and internal structural plates discussed in paragraph 1.2.

A listing of instructions for a sub-program to calculate natural frequencies is given in FORTRAN IV programming language. A main program is required to read in data and to print out calculated values of frequency. A listing of instructions is not given for the main program as the instructions required are dependent on the particular computer used.

The main program must include the COMMON statement which is written in the frequency sub-program.

IA.2 Frequency Sub-program

This sub-program solves for natural frequencies of rectangular box structures. The modes are defined by the mode numbers (m,n,q) in the three orthogonal directions. The mode numbers m,n,q are stored in variables M,N,Q respectively.

The panel data to be input for each box structure considered are values of the variables listed in Table IA.1. The plate side lengths and thicknesses for the nine cell theoretical model used are shown in Figure IA.1.

TABLE IA.1

Variable	Variable name
Cover plate side lengths	A1, A2, A3 B1, B2, B3
Cover plate thickness	TT11, TT12, TT13, TT21, TT22, TT23, TT31, TT32, TT33, TB11, TB12, TB13, TB21, TB22, TB23, TB31, TB32, TB33.
Rib and spar depth	D
Internal rib thickness	TR11, TR12, TR13, TR21, TR22, TR23, TS11, TS12, TS13, TS21, TS22, TS23.
Young's modulus for cover plates	EC
Young's modulus for internal structure	ER
Cover plate density	RHOC
Internal structure density	RHOR

Any coherent set of units in which time is expressed in seconds may be used, the frequency being obtained in Hz. It should be noted that density must be expressed in units of mass per unit volume.

On return to the main program from the frequency sub-program the natural frequency is stored in variable EXFREQ.

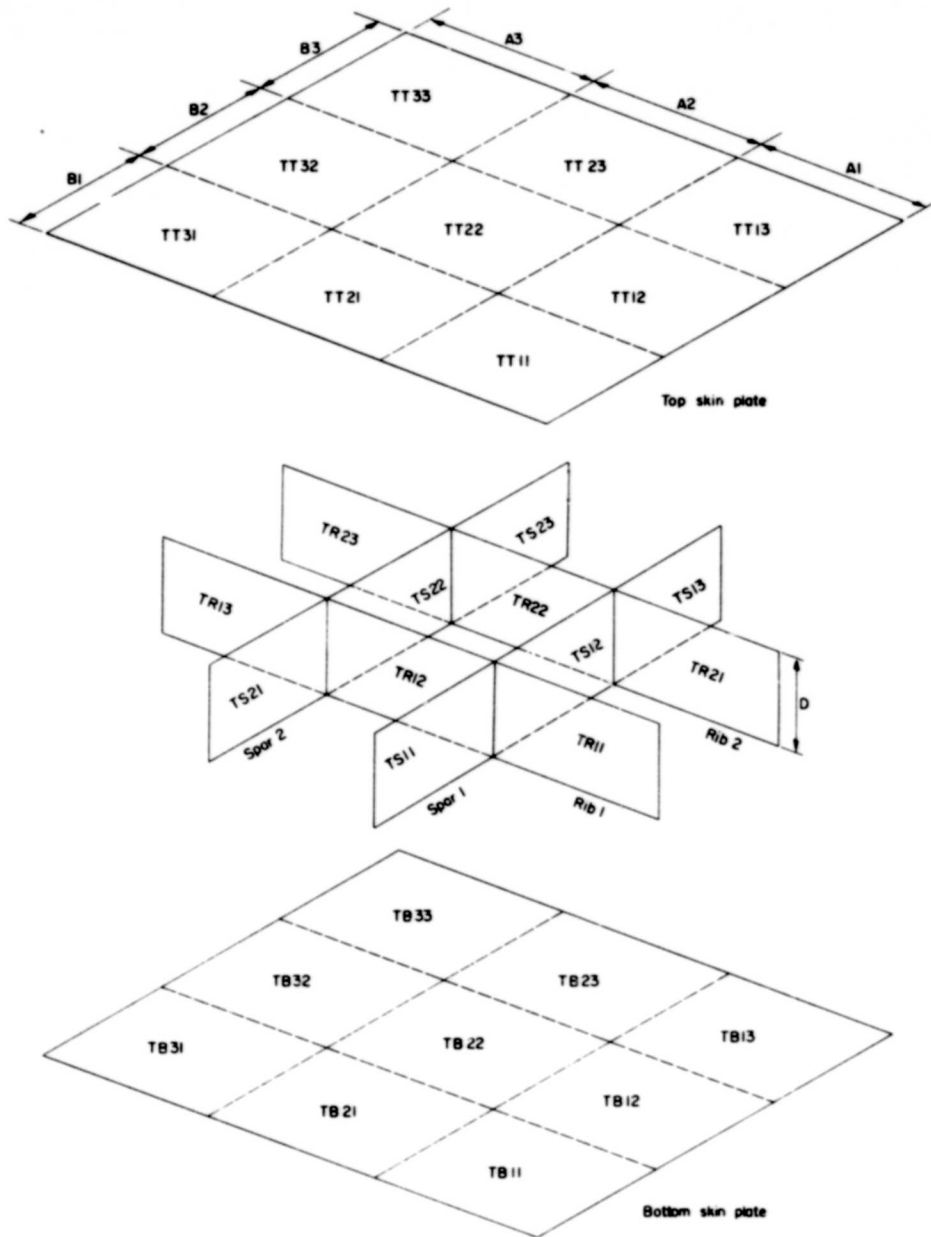


FIGURE IA | PLATE SIDE LENGTHS AND THICKNESSES FOR COMPUTER MODEL FREQUENCY ANALYSIS

SUBROUTINE FOR BOX STRUCTURE FREQUENCY

```

SUBROUTINE BOXFQ
COMMON EC, ER, RHOC, RHOR, A1, A2, A3, B1, B2, B3, D, BXFREQ, M, N, Q,
1TT11, TT12, TT13, TT21, TT22, TT23, TT31, TT32, TT33,
2TB11, TB12, TB13, TB21, TB22, TB23, TB31, TB32, TB33,
3TR11, TR12, TR13, TR21, TR22, TR23,
4TS11, TS12, TS13, TS21, TS22, TS23
REAL M, N
PNU=0.3
C
C CALCULATE MODAL STIFFNESS FOR SKIN
C
      XKC=((TT11**3+TB11**3)*A1*B1*(M*B1/(N*A1)+N*A1/(M*B1))**2+(TT13**3
1+TB13**3)*A1*B3*(M*B3/(N*A1)+N*A1/(M*B3))**2+(TT31**3+TB31**3)*A3*
2B1*(M*B1/(N*A3)+N*A3/(M*B1))**2+(TT33**3+TB33**3)*A3*B3*(M*B3/(N*A
33)+N*A3/(M*B3))**2)/(A2*B2)+((TT12**3+TB12**3)*A1*(M*B2/(N*A1)+N*A
41/(M*B2))**2+(TT32**3+TB32**3)*A3*(M*B2/(N*A3)+N*A3/(M*B2))**2)/A2
5+((TT21**3+TB21**3)*B1*(M*B1/(N*A2)+N*A2/(M*B1))**2+(TT23**3+TB23*
6*3)*B3*(M*B3/(N*A2)+N*A2/(M*B3))**2)/B2+(TT22**3+TB22**3)*(M*B2/(N
7*A2)+N*A2/(M*B2))**2
C
C CALCULATE MODAL STIFFNESS FOR RIBS AND SPARS
C
      XKR=D/(A2*B2)*((TR11**3+TR21**3)*A1*(M*D/(Q*A1)+Q*A1/(M*D))**2+(TR
112**3+TR22**3)*A2*(M*D/(Q*A2)+Q*A2/(M*D))**2+(TR13**3+TR23**3)*A3*
2(M*D/(Q*A3)+Q*A3/(M*D))**2)
      XKS=D/(A2*B2)*((TS11**3+TS21**3)*B1*(N*D/(Q*B1)+Q*B1/(N*D))**2+(TS
112**3+TS22**3)*B2*(N*D/(Q*B2)+Q*B2/(N*D))**2+(TS13**3+TS23**3)*B3*
2(N*D/(Q*B3)+Q*B3/(N*D))**2)
C
C CALCULATE MODAL MASS FOR SKIN
C
      XMC=(A1**3*(B1**3*(TT11+TB11)+B3**3*(TT13+TB13))+A3**3*(B1**3*(TT3
11+TB31)+B3**3*(TT33+TB33)))/(A2*B2)**2+B2/A2**2*(A1**3*(TT12+TB12)
2+A3**3*(TT32+TB32))+A2/B2**2*(B1**3*(TT21+TB21)+B3**3*(TT23+TB23))
3+A2*B2*(TT22+TB22)
C
C CALC MODAL MASS FOR RIBS AND SPARS
C
      XMR=D**3*(N/(Q*A2*B2))**2*(A1**3*(TR11+TR21)+A3**3*(TR12+TR22))+A3*
1*3*(TR13+TR23)
      XMS=D**3*(M/(Q*A2*B2))**2*(B1**3*(TS11+TS21)+B2**3*(TS12+TS22))+B3*
1*3*(TS13+TS23)
C
C SUM TOTAL MODAL MASS AND MODAL STIFFNESS
C
      XM=(XMC*RHOC+(XMR+XMS)*RHOR)/4.0
      XK=2.0294*(M*N)**2/(A2*B2*(1.0-PNU**2))*(XKC*EC+(XKR+XKS)*ER)
C
C CALCULATE BOX FREQUENCY
C
      BXFREQ=0.159155*SQR(XK/XM)
      RETURN
      END

```

Section 2

ESTIMATION OF R.M.S. STRESS IN INTERNAL PLATES OF A BOX STRUCTURE
SUBJECTED TO RANDOM ACOUSTIC LOADING2.1 Notation

a	spar pitch	m	in
b	rib pitch	m	in
d	depth of box	m	in
E	Young's modulus	N/m^2	lbf/in^2
f	natural frequency of response	Hz	c/s
$G_P(f)$	spectral density of external acoustic pressure at frequency f	$(N/m^2)^2/Hz$	$(lbf/in^2)^2/(c/s)$
K_n	bending stress parameter		
K_δ	damping ratio correction factor		
$L_{ps}(f)$	spectrum level of acoustic pressure at frequency f	dB	dB
p	uniform static pressure on plate	N/m^2	lbf/in^2
P_{rms}	root mean square fluctuating pressure	N/m^2	lbf/in^2
S_{rms}	root mean square stress due to acoustic loading	N/m^2	lbf/in^2
t	plate thickness	m	in
δ	damping ratio in vibrating mode		
δ_{ref}	reference damping ratio (= 0.017)		
σ	Poisson's ratio for plate material		

Suffixes

n	1-3 denotes location of plate stress (see Sketch (1))
r	denotes rib
s	denotes spar

2.2 Introduction

The first step in predicting the stress response to acoustic loading is to estimate the predominant frequency of vibration. For structures in which skin and rib plates are coupled this may be done using the procedure outlined in Section 1. The conditions for coupled vibratory response of skin and rib plates are discussed in Section 1.2. For structures where skin and rib plates are unlikely to be coupled the response frequency should be estimated for each individual plate of the box separately; the stress response is then estimated for each plate using its own response frequency. Estimates of plate natural frequencies may be obtained from Part I, Section 3 or 4 or, Part II, Section 2 of this AGARDograph.

In box structures where skin and rib plates are coupled skin and rib r.m.s. stresses, at similar plate locations, are of the same order. For uncoupled mode conditions, where ribs have relatively less bending stiffness than skins, the critical stress is likely to be that in the rib-flange radius, and when ribs are stiffer than skin plates the critical stress is likely to be in the skin at the rib-joint locations.

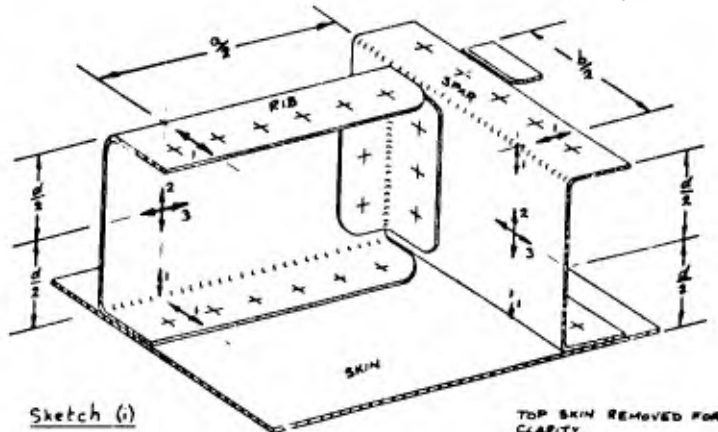
Methods for estimation of r.m.s. stress in single plates or panels, subjected to acoustic loading, are presented in Part I, Section 5 and Part III, Section 4 of this AGARDograph. It should be noted that for plates that are part of a box structure, subjected to acoustic loading on one side only, the stresses predicted by the above Sections should be multiplied by 1/3. This factor is to allow for the mechanical coupling provided by the ribs which results in the exciting energy being absorbed by two vibrating skins and interconnecting ribs.

For box structures, vibrating in a mode in which skin and rib plates are coupled, it is possible to obtain rib stresses by applying a suitable theoretical factor to the skin stress. However, it has been found that, for the limited test data available, the method suggested in this Section gives closer agreement between measured and estimated stresses than the coupled response method.

2.3 Notes

2.3.1 Data presented

This Section gives a method of estimating r.m.s. bending stresses in internal plates of box structures under the action of random acoustic loading. The boxes are assumed to be constructed from flat panels that are initially unstressed. The locations at which r.m.s. stresses are predicted are the rib and spar centres, and the edges and flanges adjoining the skin plates. The rib edge and flange stresses are at the middle of the plate side adjoining the skin and for these stresses it is implicit that the adjoining skin and rib plates are vibrating in a coupled response frequency. The locations and directions in which r.m.s. stresses are presented are shown in Sketch (i).



The r.m.s. stresses for rib and spar-web plates of a box structure that is subjected to random acoustic loading on one side are given approximately by the expression

$$S_{rms} = \frac{1}{3} \left[\frac{\pi}{4b_{ref}} f G_p(f) \right]^{1/2} \left(\frac{d}{t} \right)^2 K_n K_b,$$

when only one natural frequency is excited by the noise.

In Figure 2.1 values of K_n , the bending stress parameter, are plotted against a/d and b/d . For rib stresses, values of K_n are read corresponding to the rib aspect ratio, a/d , and for spar stresses values of K_n are read for the aspect ratio, b/d .

Figures 2.2 and 2.3 give nomographs for S_{rms} . Figure 2.3 is an extension of the r.m.s. stress range of Figure 2.2. The stress nomographs are drawn for the reference damping ratio, $b_{ref} = 0.017$; S_{rms} for other values of b is obtained by multiplying the value estimated using b_{ref} by K_b which is plotted against b in Figure 2.4. Guidance on values of b for typical aircraft structures may be found in Part III, Section 2 of this AGARDograph.

2.3.2 Assumptions in the analysis

It is assumed that each of the internal plates of a box structure may be considered in isolation under the action of the acoustic loading applied to the skin plate adjoining the internal plate under consideration.

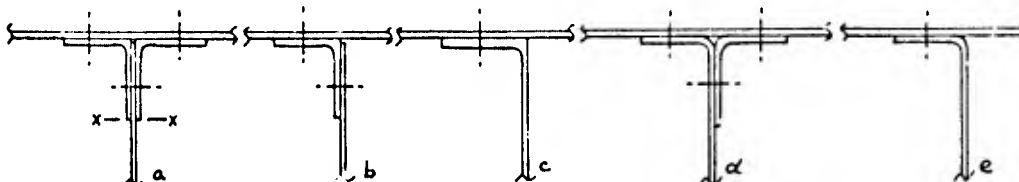
In the derivation of the nomograph it is assumed that the plate bending stress is within the linear region where it is directly proportional to the normal pressure, that is p/E less than about $20(t/d)^4$ (see Reference 2.6.8). In calculating K_n the value of σ was assumed to be 0.3; use of this value gives a sufficiently accurate stress for all common structural metallic materials.

The pressure is assumed to be uniform and in-phase over the whole of each individual skin plate and the spectrum level of acoustic pressure is assumed to be constant over the range of frequencies close to the natural frequency of response of the box structure. If the response frequency of the structure is not known, for conventional aircraft structures without special damping treatment the first natural frequency obtained from Section 1 of this AGARDograph should be used.

When box structures do not vibrate in a mode in which skin and rib plates are coupled, the response frequencies of the rib and skin plates may be such that there is a significant difference between the spectral densities of acoustic pressure at the two frequencies. This condition may occur, for example, in boxes with deep ribs. Estimated r.m.s. stresses, for such cases, should be used with caution when predicting fatigue life. There are insufficient test data for this type of box structure to provide guidance for these cases.

Due to mechanical coupling between skin plates, provided by the ribs and spars, it has generally been found that, for box structures subjected to noise on one side only, the r.m.s. stress response on the internal plate edge and flange adjoining the skin plate remote from the excitation agrees closely with that obtained from those adjoining the skin plate directly excited by the noise. For box structures subjected to noise on both skin plates, such as aircraft fin boxes, it is recommended that the calculated value of S_{rms} , obtained from this data sheet, should be multiplied by 1.4.

The rib, or spar, edge stresses obtained from this Section are nominal values in the plain material adjacent to the bend-radius or joint. The appropriate stress to be used in estimating fatigue life, from Part II Section 1 or Part IV Section 3 of this AGARDograph (or other endurance data), is dependent on the detail design of the joint used. Typical riveted skin/rib joints, without jointing compound, are shown in Sketch (ii). Likely critical regions on the ribs for these joints under acoustic loading are Section XX for a, the rivet holes for b and d and the rib flange bend radius for c and e.



Sketch (ii)

This data sheet may be used to obtain first approximations to the r.m.s. stresses in box structures with stiffened skin plates. In these cases an effective thickness is used which should be that necessary to give the same frequency as that of the stiffened plate.

2.4 Calculation Procedure

2.4.1 Procedure for estimating S_{rms}

- (i) If the response frequency is not known, estimate the lowest natural frequency of the box using Section 1.
- (ii) Obtain the value of spectrum level of acoustic pressure $L_{ps}(f)$ at the response frequency. If only the band pressure level is known, it is first corrected to pressure spectrum level (unit bandwidth) using Reference 2.6.6. The reference pressure for sound pressure level is $20 \mu N/m^2$.
- (iii) For each rib plate to be considered calculate the parameters a/d and b/d respectively and, from Figure 2.1, read the appropriate values of K_n .
- (iv) Calculate the plate parameters d/t_r and d/t_s and, for each plate location and stress direction, read the values of S_{rms} from Figures 2.2 or 2.3. The nomographs are entered at a value of $L_{ps}(f)$, each quadrant being used in turn in the direction indicated through ranges of d/t , K_n and f .
- (v) For values of b other than 0.017, factor the estimated value of S_{rms} by K_b obtained from Figure 2.4.

2.4.2 The loading

Within the nomograph the spectrum sound pressure level is converted into the spectral density of acoustic pressure. The spectrum sound pressure level is converted into the root mean square fluctuating pressure in units of $(N/m^2)/Hz$ (see expression below or reference 2.6.7) and then squared giving a value in units of $(N/m^2)^2/Hz^2$. Since unit bandwidth is used this is numerically equal to the spectral density of acoustic pressure $G_p(f)$ in units of $(N/m^2)^2/Hz$.

Using SI units,

$$L_{ps}(f) = 20(\log_{10} p_{rms} + 4.70).$$

If $L_{ps}(f)$ is required in British units of $(lb/in^2)^2/(c/s)$ it is given by

$$L_{ps}(f) = 20(\log_{10} p_{rms} + 8.54).$$

2.5 Comparison with Measured Data

Figure 2.5 shows a comparison of estimated and measured r.m.s. stresses in internal plates of box structures using the lowest natural frequency for each box calculated by the method presented in Section 1 of this AGARDograph. In calculating these stresses the damping ratio was assumed to be $\delta_{ref} (= 0.017)$.

In Figure 2.6 a similar comparison of estimated and measured stresses is presented, the estimated stress being obtained using the measured plate response frequency and, where available, the measured damping ratio for the box structures. All boxes considered are idealised structures, i.e. without cut-outs or stiffeners between ribs and spars.

2.6 Derivation and References

Derivation

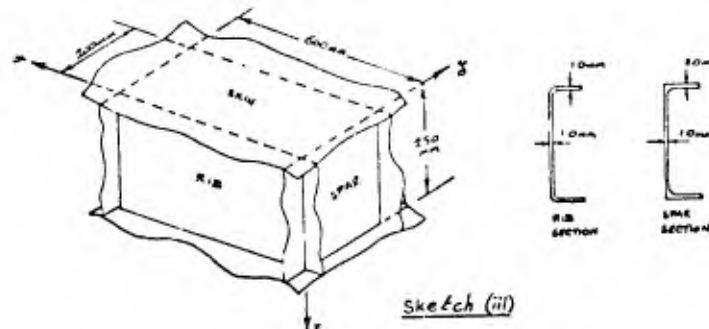
- 2.6.1 Timoshenko, S. Theory of plates and shells. Second Edition, McGraw Hill, New York, 1959.
- 2.6.2 Woinowsky-Krieger, S.
- 2.6.2 Clarkson, B.L. Stresses in skin panels subjected to random acoustic loading. J.R. aeronaut. Soc., Vol. 72, No. 695, pp.1000-1010, November 1968.
- 2.6.3 Barrett, G.W. Fatigue and response testing of riveted joints in panels subjected to wide band loading in the B.A.C. (Weybridge) high intensity noise facility. British Aircraft Corporation (Weybridge) Acoustics Rep. No. 048, Part 2. Work under Ministry of Technology Contract KS/1/0504/CB.43A2, November 1970.
- 2.6.4 Rudde, F.F. Acoustic fatigue of aircraft structural component assemblies. Air Force Flight Dynamics Lab. Rep. AFFDL-TR-71-107, February 1972.
- 2.6.5 Clarkson, B.L. Estimates of the response of box type structures to acoustic loading. Paper 10 of Proceeding of Symposium on Acoustic Fatigue, Toulouse, September 1972, AGARD-CP-113, May 1973.

References

- 2.6.6 - Bandwidth correction. Engineering Sciences Data Item No. 66016, February 1966.
- 2.6.7 - The relation between sound pressure level and r.m.s. fluctuating pressure. Engineering Sciences Data Item No. 66018, February 1966.
- 2.6.8 - Elastic direct stresses and deflection for flat rectangular plates under uniformly distributed normal pressure. Engineering Sciences Data Item No. 71013, May 1971.

2.7 Example

It is required to estimate the edge and flange stresses on the rib and spar, at the midposition between spars and ribs respectively, and the rib and spar centre stresses for the box structure shown in Sketch (iii). The structure is exposed to jet noise on the upper side only.



The variation of sound pressure level over a range of frequencies is given in the table, sound pressure levels being 1/3 octave band levels.

sound pressure level dB	134	135	135.5	135.5	135
frequency Hz	50	75	100	200	300

Dimensions of the box structure are given in Sketch (ii). Material properties are as follows:

$$E_r = E_s = 70\,000 \text{ MN/m}^2, \quad \nu = 0.3, \quad b = 0.019.$$

The frequency of response of the box structure is 92 Hz and this vibration mode is one in which the skin plates and internal plates are coupled.

By interpolation from the table the 1/3 octave band pressure level at 92 Hz is 135 dB.

From Reference 2.6.6, $L_{ps}(f) = 135 - 13.4 = 122 \text{ dB}.$

Now $\frac{a}{d} = \frac{600}{250} = 2.4$

and $\frac{b}{d} = \frac{200}{250} = 0.80.$

Using these ratios the values of K_n listed in the table are found from Figure 2.1.

For all locations on the rib $\frac{d}{t} = \frac{250}{1.0} = 250.$

For the spar centre and edge stresses $\frac{d}{t} = \frac{250}{1.0} = 250,$

and for the spar flange $\frac{d}{t} = \frac{250}{2.0} = 125.$

From Figure 2.2, entering the nomograph at 122 dB the values of S_{rms} for the reference damping ratio are found.

From Figure 2.4 for $b = 0.019$ $K_b = 0.95.$

Hence the required values of S_{rms} are as listed in the table.

Component	Location	K_n	d/t	S_{rms} ($b = 0.017$) MN/m ²	S_{rms} ($b = 0.019$) MN/m ²
Rib	edge	0.50	250	17.1	16.2
	flange	0.50	250	17.1	16.2
	centre in x-direction	0.170	250	5.8	5.5
	centre in z-direction	0.458	250	15.7	14.9
Spar	edge	0.214	250	7.3	7.0
	flange	0.214	125	1.8	1.7
	centre in y-direction	0.186	250	6.4	6.0
	centre in z-direction	0.140	250	4.8	4.6

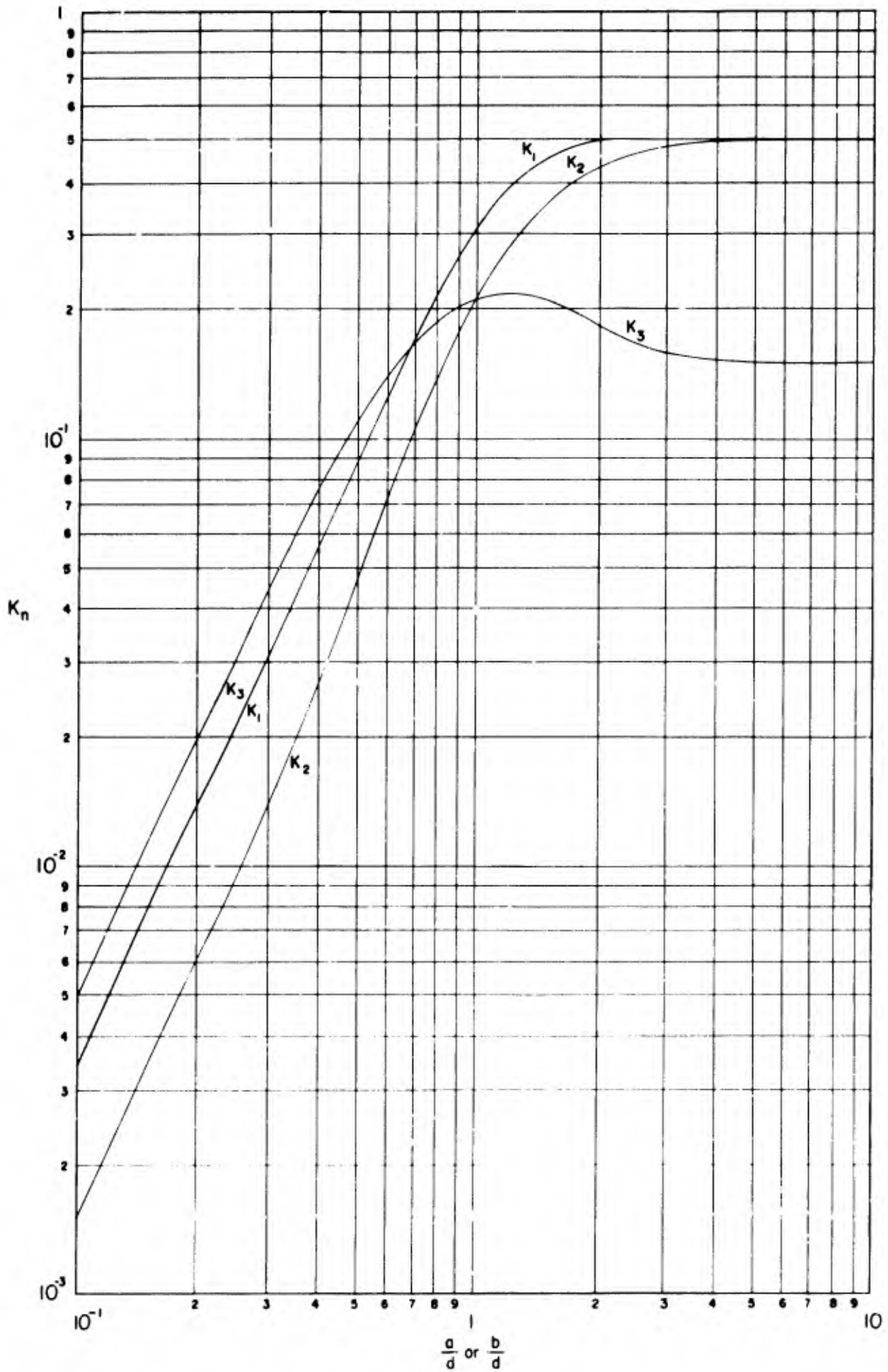


FIGURE 2.1 BENDING STRESS PARAMETER FOR RIB AND SPAR STRESSES

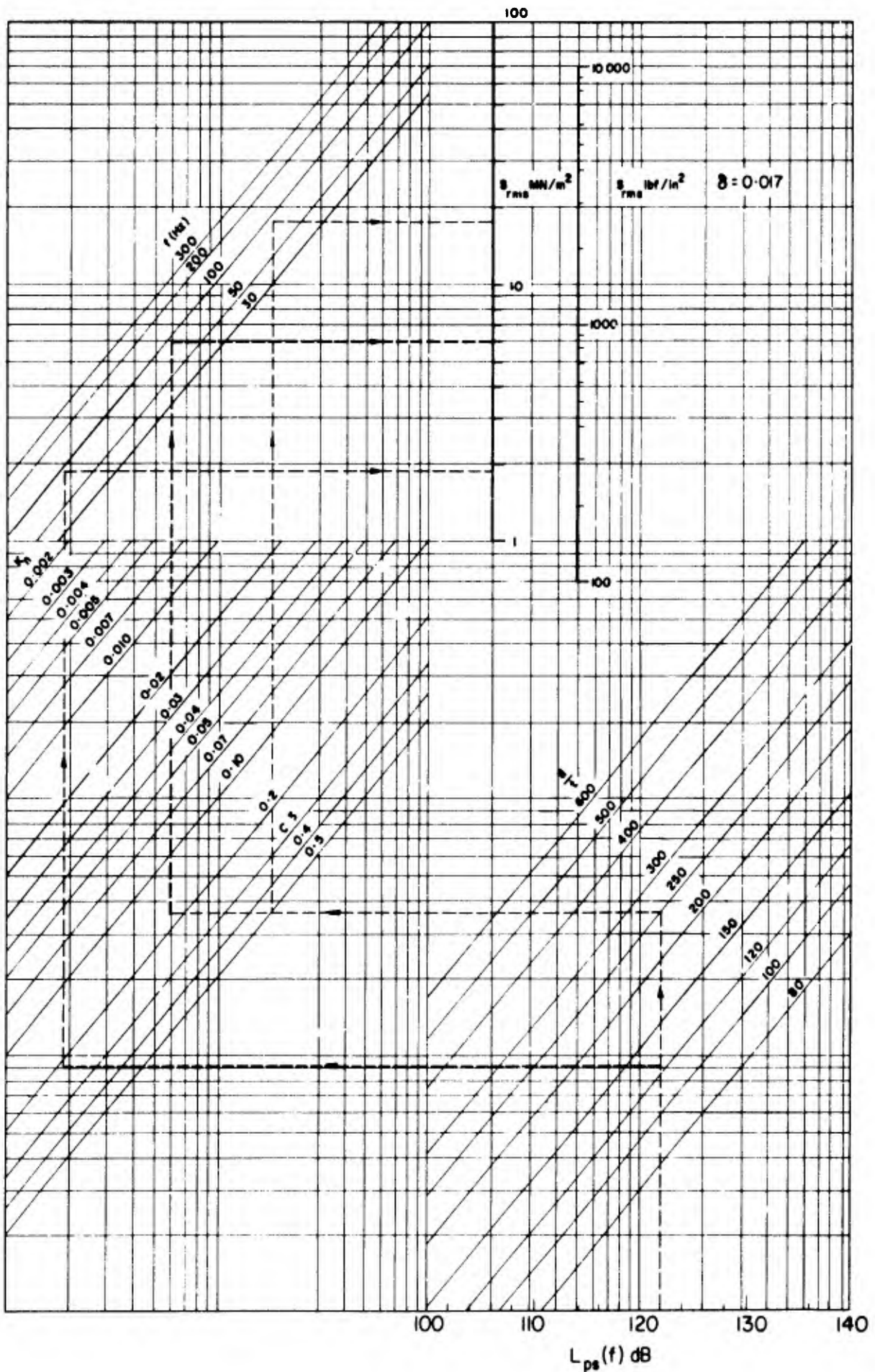


FIGURE 2.2 STRESS NOMOGRAPH

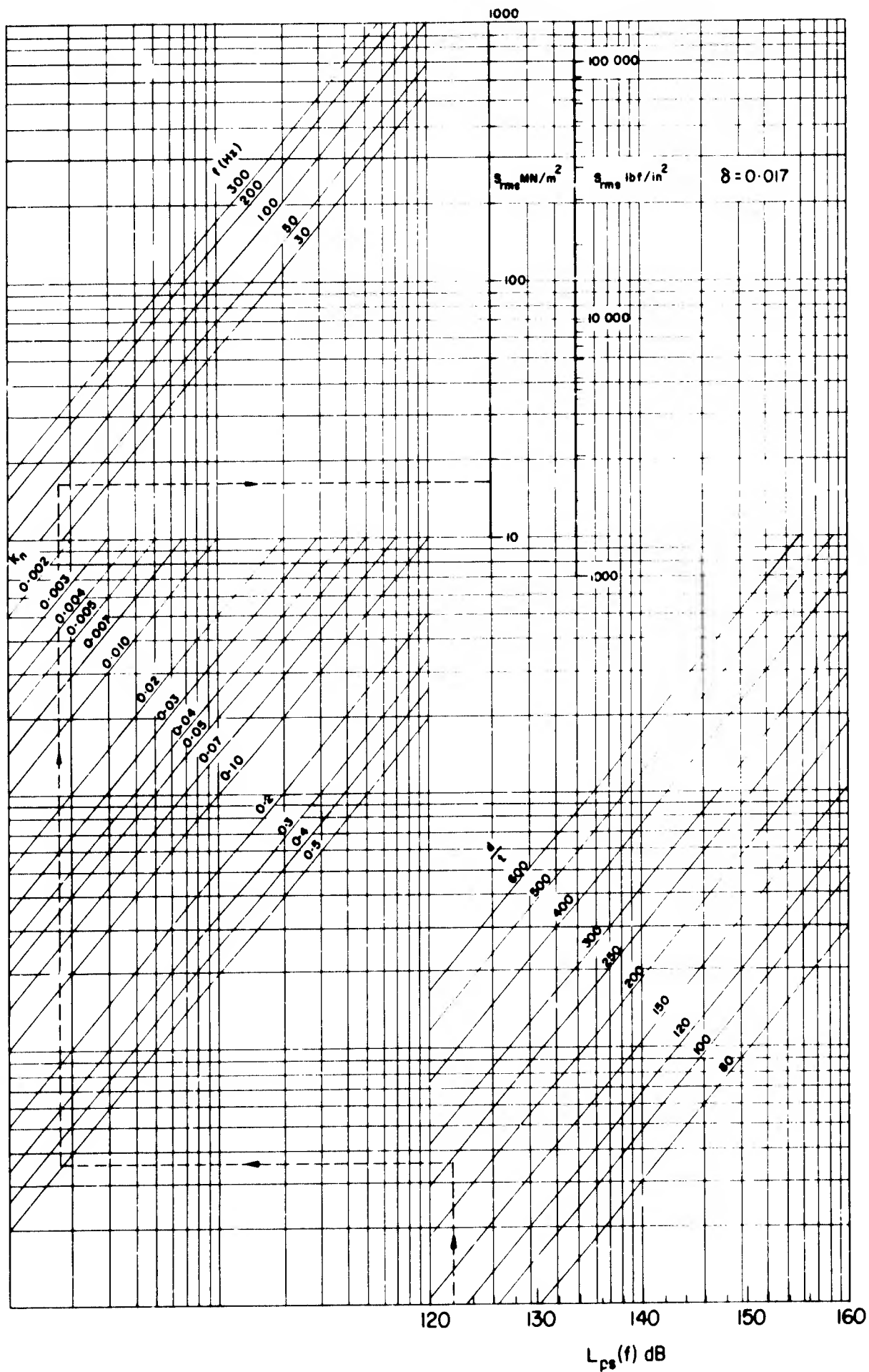


FIGURE 2.3 STRESS NOMOGRAPH

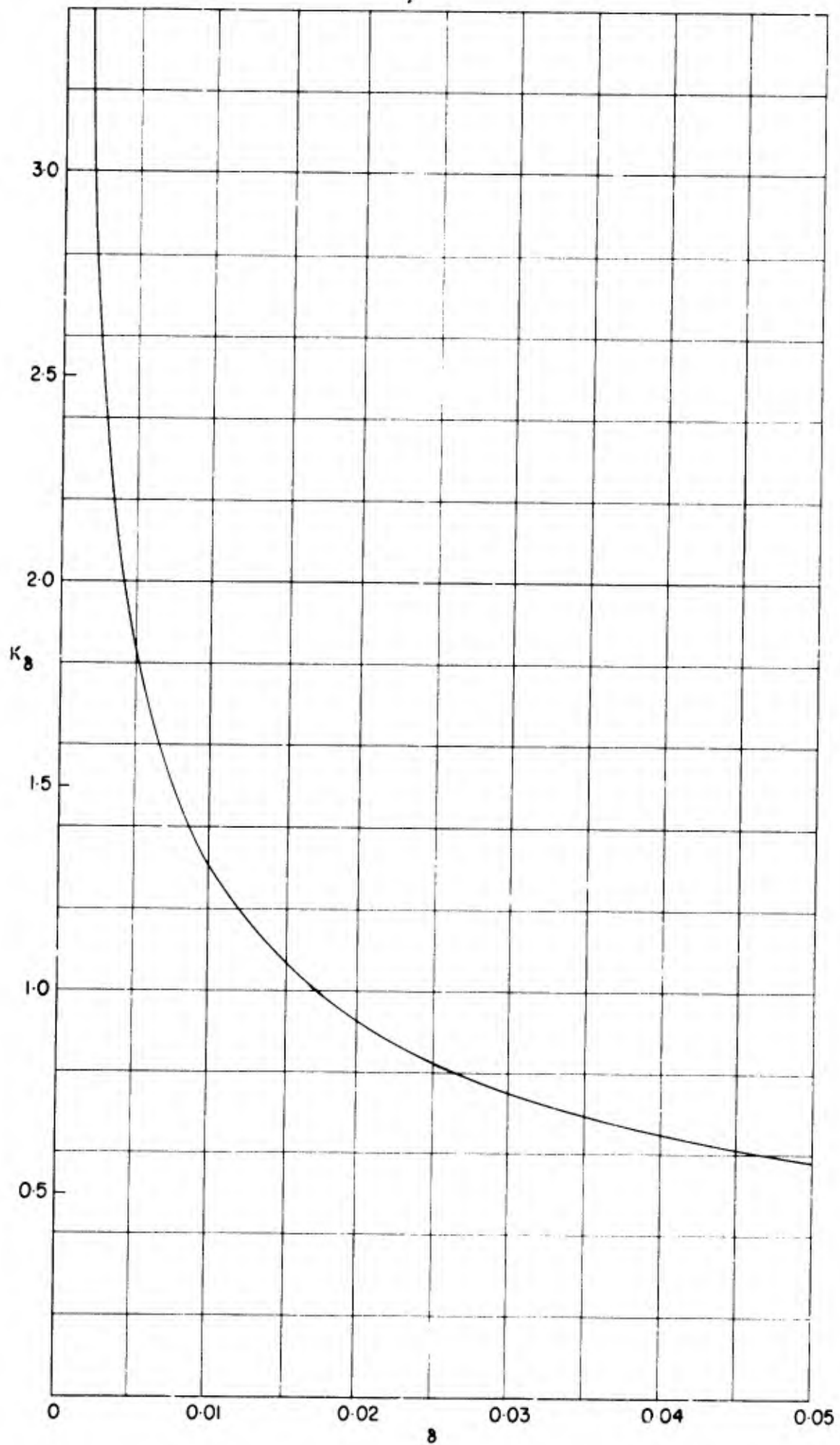


FIGURE 2.4 DAMPING RATIO CORRECTION FACTOR

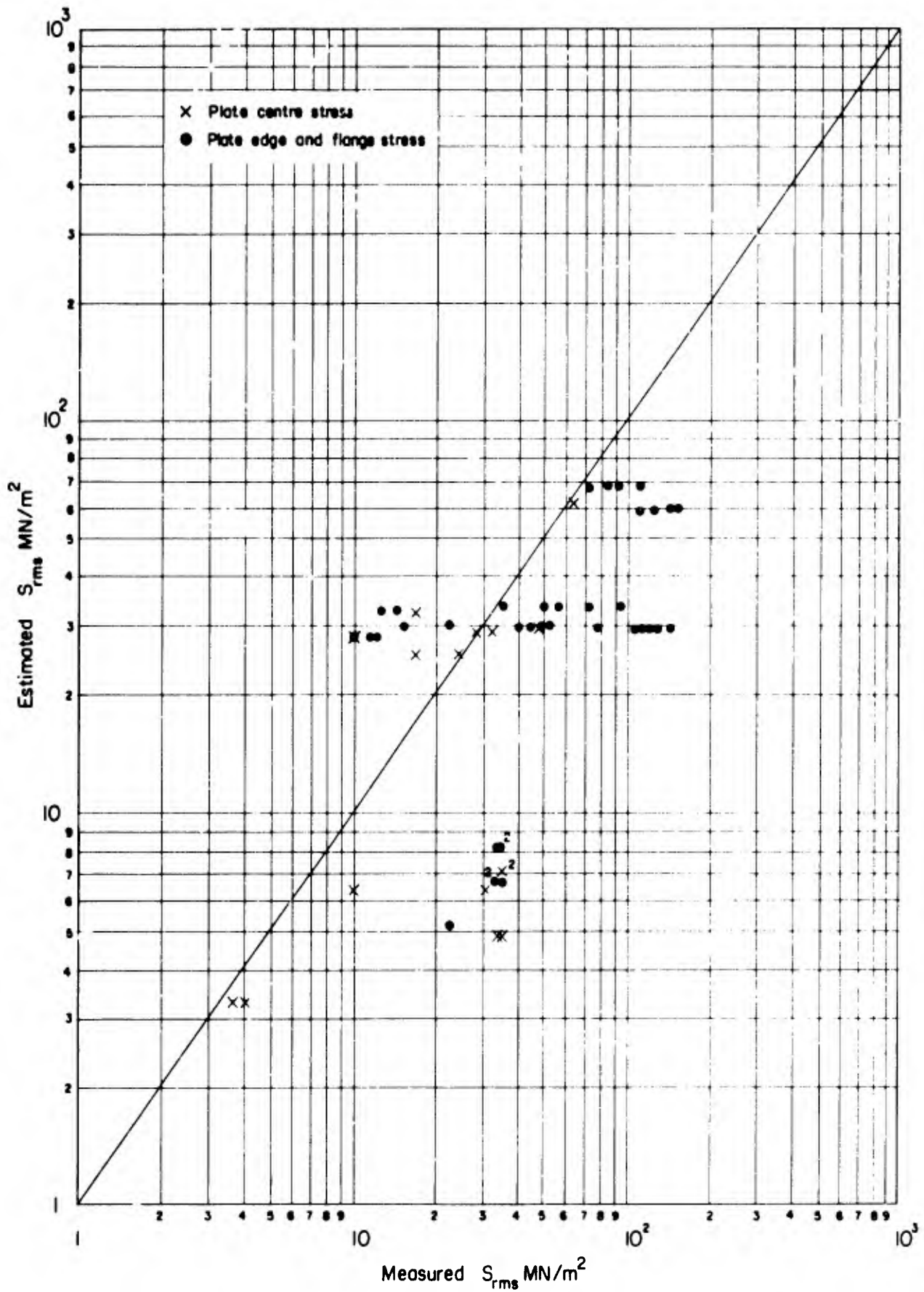


FIGURE 2.5 COMPARISON OF ESTIMATED AND MEASURED STRESS USING CALCULATED FREQUENCY AND $\delta=0.017$ FOR STRESS ESTIMATION

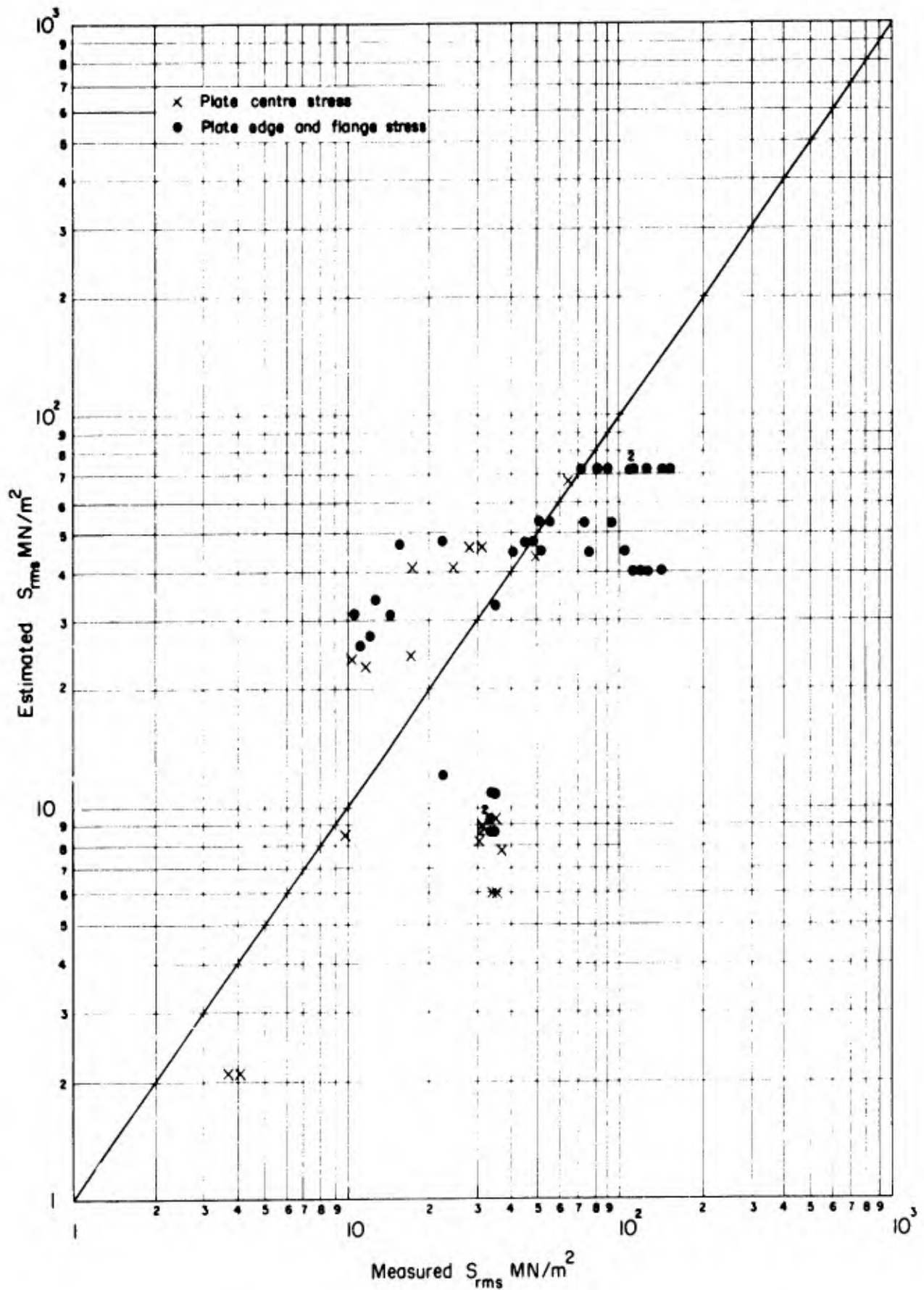


FIGURE 2.6 COMPARISON OF ESTIMATED AND MEASURED STRESS USING MEASURED FREQUENCY AND DAMPING RATIO FOR STRESS ESTIMATION

Section 3

ESTIMATION OF SOUND PRESSURE LEVELS DUE TO BUZZ-SAW NOISE WITHIN THE INTAKE
DUCT OF A SUPERSONIC FAN OR COMPRESSOR

3.1 Introduction

Buzz-saw tones (also known as combination tones) are generated in a fan or compressor when the rotor blade Mach number relative to the incident airstream exceeds unity. In a practical rotor the resulting shock waves propagate from the rotor face with differing intensities, spacing and angles because of geometric and aeroelastic differences between individual blades. (See Figure 1) These variations can give rise to tones at low frequencies that are integral multiples of shaft frequency, as well as at blade passing frequency, which can be sufficiently intense to cause acoustic fatigue damage within the intake duct.

3.2 Notation

B	number of fan or compressor blades		
E	shaft rotational frequency	Hz	Hz
f	frequency of buzz-saw tone	Hz	Hz
K	shaft order number, f/E		
K_{co}	shaft order number at cut-off		
L_K	average sound pressure level of tone of shaft order K in intake duct at distance x from compressor face, $L_x + L_M + L_B + L_{K\sigma}$	dB	dB
L_B	component of L_K dependant upon the number of blades and surviving shocks	dB	dB
$L_{K\sigma}$	component of L_K dependant on shaft order number and standard deviations of shock spacing and amplitude	dB	dB
L_M	component of L_K dependant upon Mach Number of incident flow on the blades	dB	dB
L_x	component of L_K dependant upon x/R	dB	dB
M_A	intake axial flow Mach number		
M_T	tangential Mach number at blade tip		
N	number of shock waves per shaft revolution surviving at duct plane under consideration		
p_0	static pressure in intake duct	N/m^2	lbf/ft^2
p_{ref}	reference pressure for decibel scale, taken as $20\mu N/m^2$ ($0.42 \times 10^{-6} lbf/ft^2$)	N/m^2	lbf/ft^2
R	tip radius of fan or compressor	m	ft
x	axial distance upstream of compressor face	m	ft
γ	ratio of specific heats for air (taken as 1.4)		
σ_A	standard deviation of normalised shockwave ampli.		
σ_E	standard deviation of normalised shockwave spacing.		

Both SI and British units are quoted, but any coherent system of units may be used.

3.3 Notes

3.3.1 Summary of Method

The sound pressure level at the duct wall at distance x from the compressor face for any buzz-saw tone is estimated from the sum $L_K = L_x + L_M + L_B + L_{K\sigma}$.

The components L_x , L_M and L_B are plotted in Figures 3.2, 3.3 and 3.4 against the appropriate engine parameters. These components are constant at a given station in the duct for a given fan and running conditions. The component $L_{K\sigma}$ is plotted in Figures 3.5 and 3.6. This component defines the shape of the envelope of the peaks of the buzz-saw tone spectrum and must be evaluated for each tone required. Figure 3.5 relates to tones at integer multiples, K, of shaft frequency and Figure 3.6 to tones at integer multiples of blade passage frequency.

Tones below a critical cut-off frequency do not propagate efficiently along the duct. Figure 3.7 gives the value of the shaft-order K_{co} at this cut-off. Except very close to the compressor face, the sound pressure levels at frequencies less than K_{co} may be expected to be much lower than calculated.

It is assumed that values of B , K , M_A , M_T , p_0 , R and x are known or have been chosen. The remaining parameters required to estimate L_K are the standard deviations of shock-wave amplitude and spacing, σ_A and σ_E , and the number of surviving shockwaves N . The values of these parameters for a given fan are not always available. Guidance on their estimation is given in Section 3.3.3.

3.3.2 Assumptions and limitations

No allowance is made for the effect of any acoustic lining of the duct. It is assumed that the inlet flow is axial and uniform across the intake duct, which has parallel walls and no intake guide vanes. The data apply at values of x greater than about one blade spacing. Closer to the rotor face the sound energy is concentrated at blade-passage frequency and tends to a value dependant on the initial shock strength at the rotor face.

The estimation method shows good agreement with experimental results measured within the duct within a few blade spacings of the compressor face. For fans with short ducts (duct length less than fan diameter) measurements in the far-field, outside the duct, are also consistent with estimations. There are indications that for certain fans with intake ducts longer than the fan diameter the attenuation in the duct may be greater than predicted by this method.

In Figure 3.6, a value of $\sigma_A = 0.1$ has been assumed. Departures from this value have a negligible effect on the value of $L_{K\sigma}$ for integral values of K/N . It is assumed that the distributions of shock spacing and amplitude are statistically normal.

Because the noise at shaft-order frequencies is caused by small differences between individual rotor blades, each rotor has its own unique spectrum of buzz-saw levels. The method can therefore give only typical levels and should not be expected to produce precise agreement with any one set of measured results.

3.3.3 Statistical parameters of shock-waves

As buzz-saw tones are dependant on geometric and aeroelastic differences between individual blades, this data sheet is based on a statistical, theoretical treatment incorporating the statistical characteristics σ_A , σ_E and N of the shock-waves of a particular fan.

It is recommended that, if possible, values of these parameters should be inferred from test data. The following guidance can be given. The exact value of σ_A has relatively little effect on the sound pressure level of the buzz-saw tones except at low shaft orders, or when σ_E is small.

(See Figure 3.5). The value of σ_A increases from a very small value close to the rotor face typically up to value of 0.15 to 0.2 at large values of x . In the absence of test data it is recommended that σ_A should be assumed equal to 0.1, unless tones at low multiples of shaft

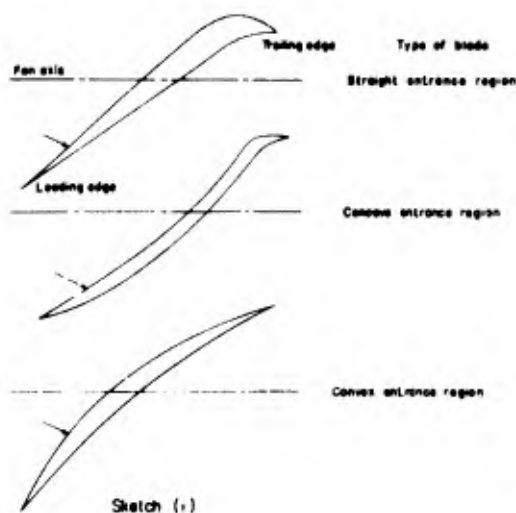
frequency are likely to be particularly critical as a source of acoustic fatigue damage, when it is safer to allow for a value of σ_A up to 0.2.

The value of σ_E increases from a small value close to the rotor face up to a value typically between 0.2 and 0.3 at the duct exit.

For purposes of estimating N it is recommended that the following values are taken (Derivation 3.3):-

straight or slightly concave entrance region blades $N = \frac{B}{2}$,

convex entrance regions blades $N = B$. (See sketch (i)).



3.4 Derivation

The Figures are based on the following expressions.

Figure 2.

$$L_x = 20 \log \left[\frac{Y}{Y+1} \frac{P_o}{P_{ref}} \frac{\pi R}{x} \right] + 10 \log \frac{\pi}{6}$$

Figure 3.

$$L_M = 10 \log \frac{4 (M_A^2 + M_T^2 - 1)}{(M_A^2 + M_T^2)^4} \left[M_A (M_A^2 + M_T^2 - 1)^2 - M_T \right]^4$$

Figure 4.

$$L_B = 30 \log \left[\frac{1}{B} \cdot \frac{B}{N} \right]$$

Figure 5.

$$L_{Kc} = 10 \log \frac{4}{\eta^4} \left[\eta^2 + 2(1 - \cos \eta) - 2\eta \sin \eta \right] (1 + 6\sigma_E^2) \left[1 + \sigma_A^2 - \exp(-\sigma_E^2 \eta^2) \right],$$

where $\eta = 2\pi K/N$.

Figure 6.

$$L_{K\sigma} = 10 \log \frac{4}{\eta^4} \left[\eta^2 + 2(1 - \cos \eta) - 2\eta \sin \eta \right] (1 + 6\sigma_E^2) \left[1 + \sigma_A^2 + (B-1) \exp(-\sigma_E^2 \eta^2) \right],$$

where $\eta = 2\pi K/N$.

Figure 7.

$$K_{co} = 0.77 \left[\frac{M_T}{(1 - M_A^2)^2 \left[1 - 0.1 \exp 23.03 \left\{ 1 - (M_A^2 + M_T^2)^2 \right\} \right]} - 1 \right]^{-\frac{3}{2}}$$

- | | | |
|-------|--------------------------------|---|
| 3.4.1 | Morfev, C.L.
Fisher, M.J. | Shock wave radiation from a supersonic ducted rotor.
Aeronaut. J. Vol.74, No.715, July 1970. |
| 3.4.2 | Philpot, M.G. | The buzz-saw noise generated by a high duty transonic compressor.
Journal of Engineering for Power, January 1971. |
| 3.4.3 | Burdshall, E.A.
Urban, R.H. | Fan-compressor noise: prediction, research, and reduction studies.
FAA-RD-71-73. February 1971. |
| 3.4.4 | Pickett, G.F. | The prediction of the spectral content of combination tone noise.
AIAA/SAE 7th Propulsion Joint Specialist Conference
AIAA paper No. 71-730, June 1971. |

3.5 Example

Determine the spectrum of buzz-saw tones up to 10 kHz for a fan with convex blades in the entrance region having the following dimensions and running conditions.

$$\begin{aligned}
 B &= 35 & R &= 3.5 \text{ ft} \\
 M_A &= 0.45 & x &= 4.0 \text{ ft} \\
 M_T &= 1.1 & \sigma_A &= 0.1 \\
 p_0 &= 1900 \text{ lbf/ft}^2 & \sigma_E &= 0.2
 \end{aligned}$$

From Figure 3.2, for $x/R = 1.14$ and $p_0 = 1900 \text{ lbf/ft}^2$,

$$L_x = 194.4 \text{ dB.}$$

From Figure 3.3, for $M_A = 0.45$ and $M_T = 1.1$,

$$L_M = 7.5 \text{ dB.}$$

From Figure 3.4, for $B/N = 1$ (appropriate to convex blades in the entrance region, according to Section 3.3.3) and $B = 35$

$$L_B = -46.3 \text{ dB.}$$

Then $L_x + L_M + L_B = 194.4 - 7.5 - 46.3 = 140.6 \text{ dB.}$

Referring to Figure 3.5, a range of values of K is chosen.

To obtain buzz-saw frequencies up to $f = 10 \text{ kHz}$ it is necessary to take a range of K up to about $\frac{10 \text{ kHz}}{E} = \frac{10 \text{ kHz}}{56 \text{ Hz}} \approx 180$.

From Figure 3.5 the following table is constructed, using values of $\sigma_A = 0.1$, $\sigma_E = 0.2$ and $N = B = 35$.

The value of L_K is then obtained from $L_K = L_x + L_M + L_B + L_{K\sigma} = 140.6 + L_{K\sigma}$.

K	$\frac{K}{N}$	$L_{K\sigma}$	L_K
1	0.0286	-18.5	122.1
2	0.0571	-17.3	123.3
3	0.0857	-15.8	124.8
5	0.143	-13.1	127.5
10	0.286	-8.7	131.9
20	0.571	-6.1	134.5
30	0.857	-8.0	132.6
50	1.429	-12.5	128.1
100	2.857	-17.7	122.9
140	4.00	Since K/N is an integer, see Figure 3.6.	
180	5.14	-23.4	117.2

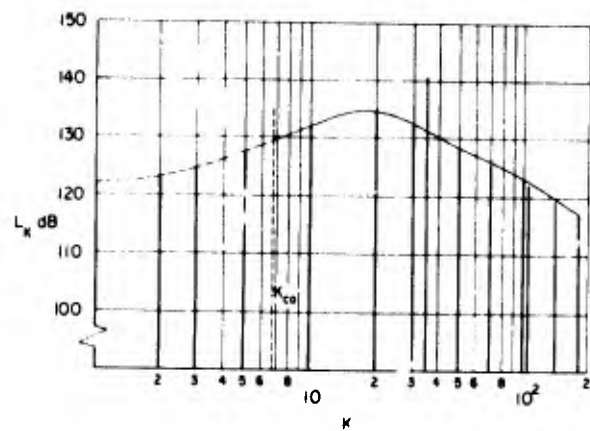
From Figure 3.6, the following values are obtained.

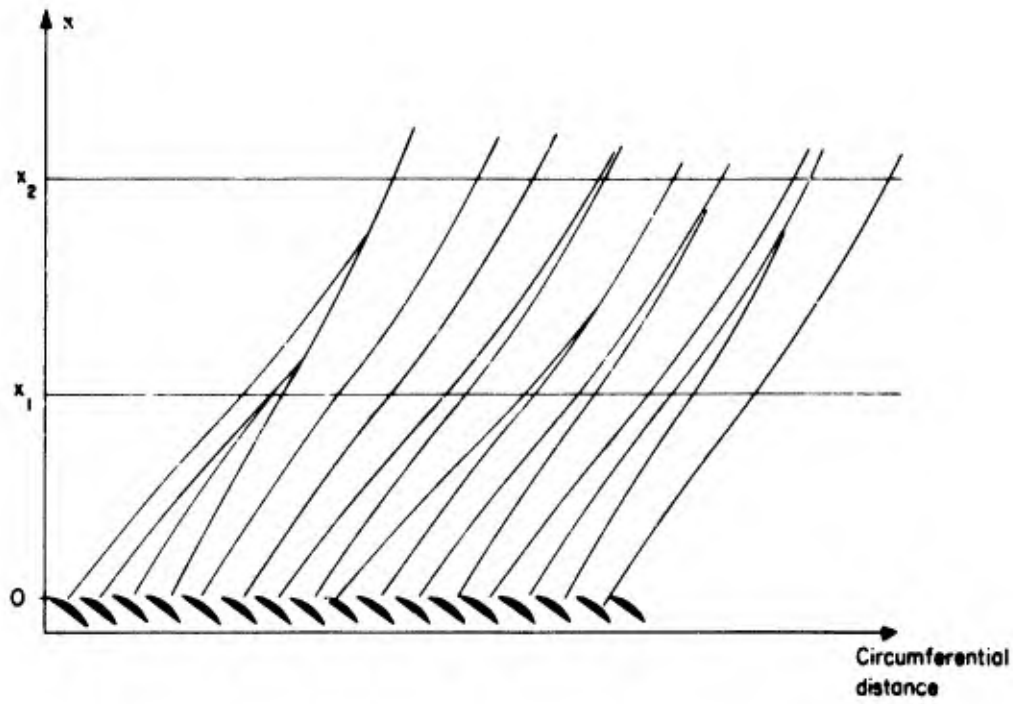
K	$\frac{K}{N}$	$L_{K\sigma}$	L_K
35	1	+0.0	140.6
70	2	-14.7	125.9
105	3	-18.5	122.1
140	4	-21.0	119.6

From Figure 3.7, for $M_A = 0.45$ and $M_T = 1.1$,

$$K_{co} = 6.8.$$

The following envelope of buzz-saw tones is drawn from the above tables, ignoring the tones for K less than K_{co} .

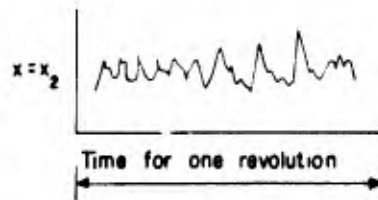
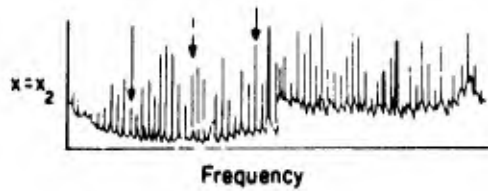
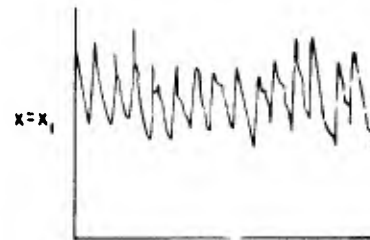
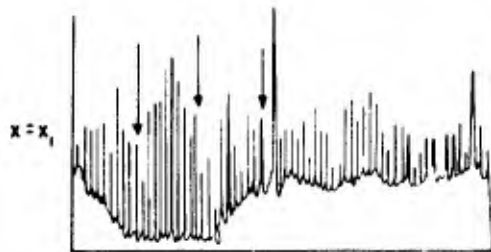
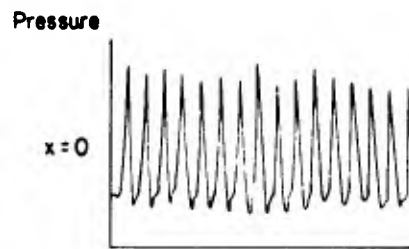
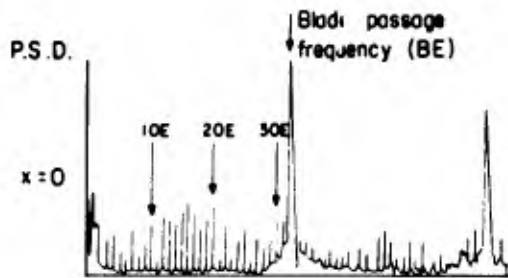




Shock wave pattern from a real fan

Power spectral density vs frequency

Pressure vs time



X = Distance upstream from rotor
 B = Number of rotor blades
 E = Rotor shaft speed

FIGURE 3.1 'BUZZ-SAW' CHARACTERISTICS

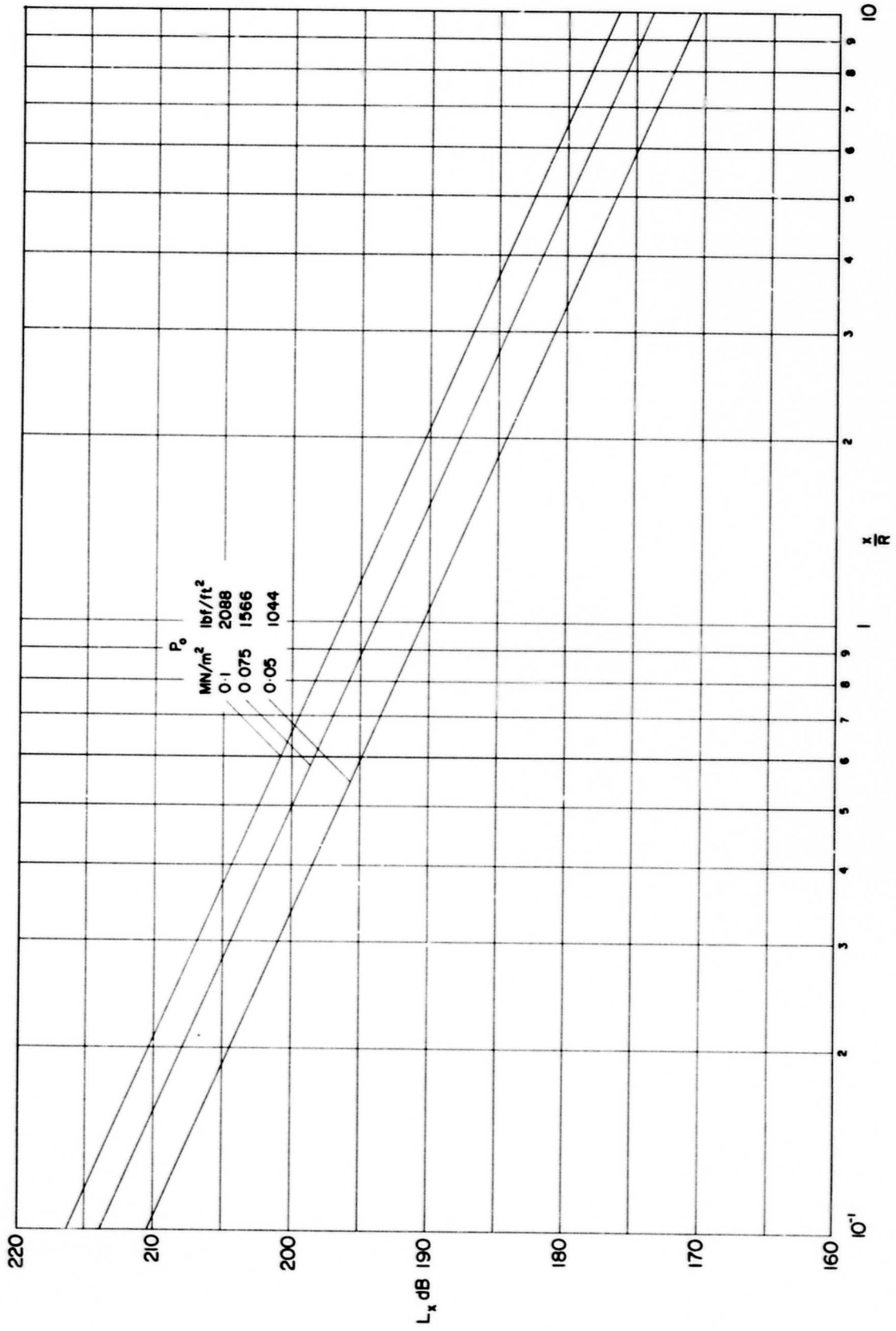


FIGURE 3.2 COMPONENT OF SOUND PRESSURE LEVEL, L_x

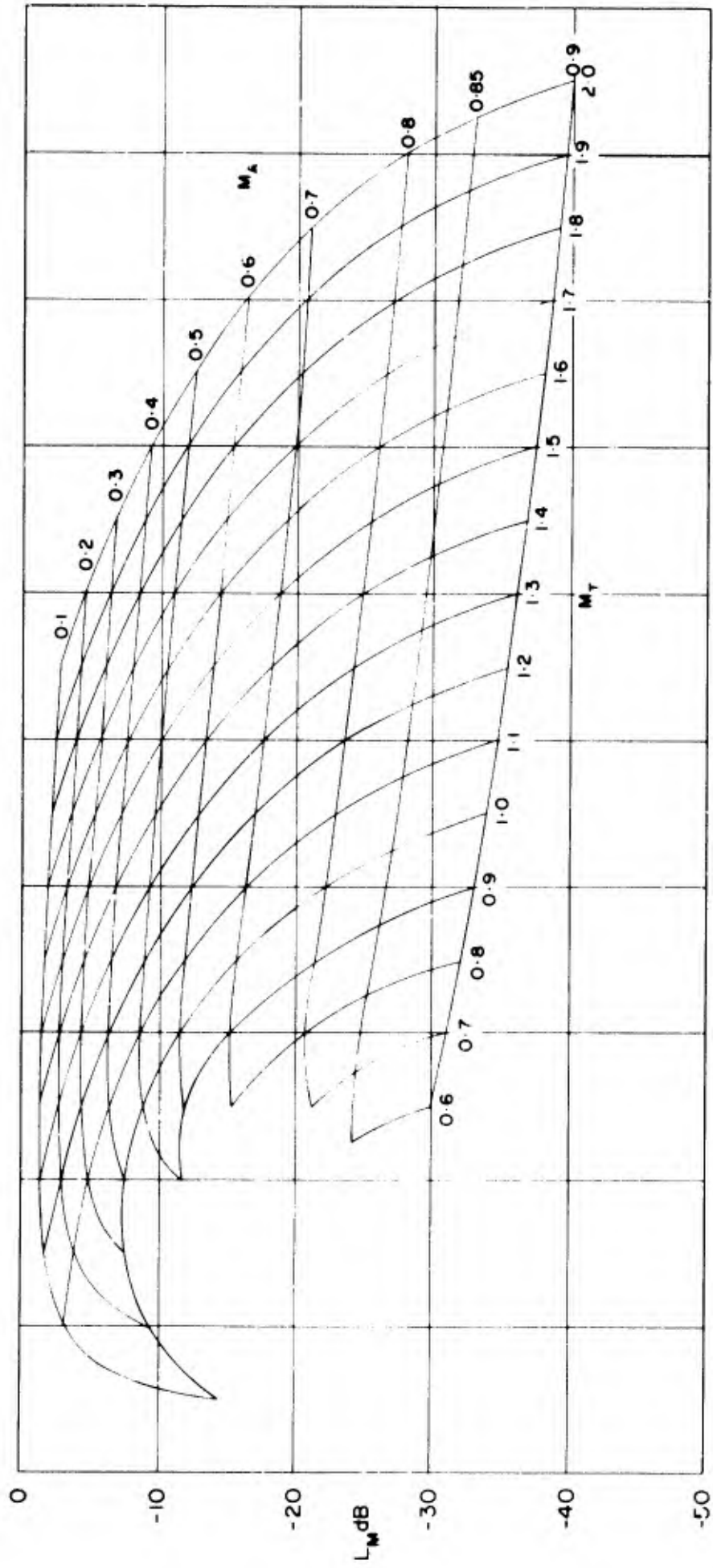
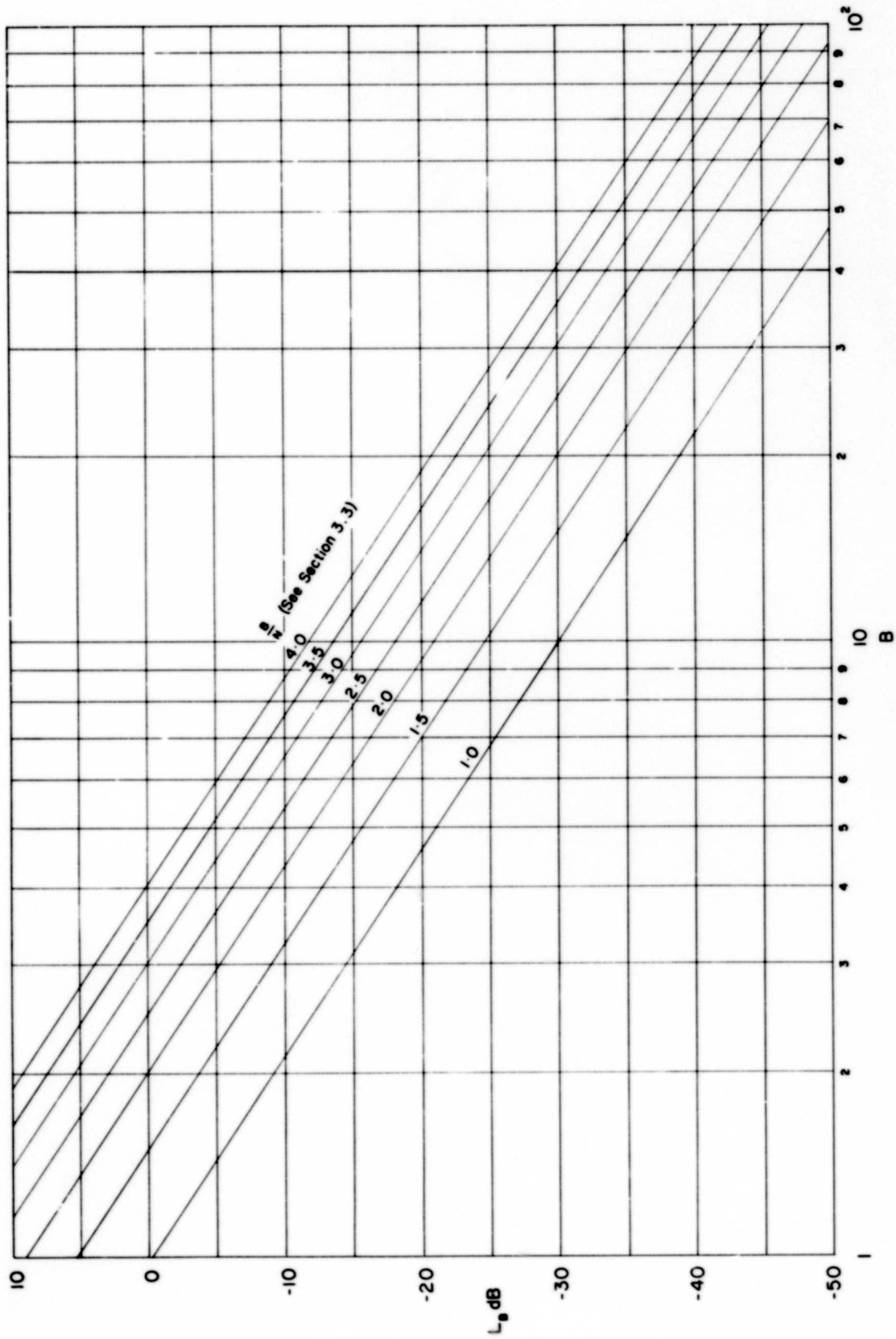


FIGURE 3.3 COMPONENT OF SOUND PRESSURE LEVEL, L_M

FIGURE 3.4 COMPONENT OF SOUND PRESSURE LEVEL, L_B

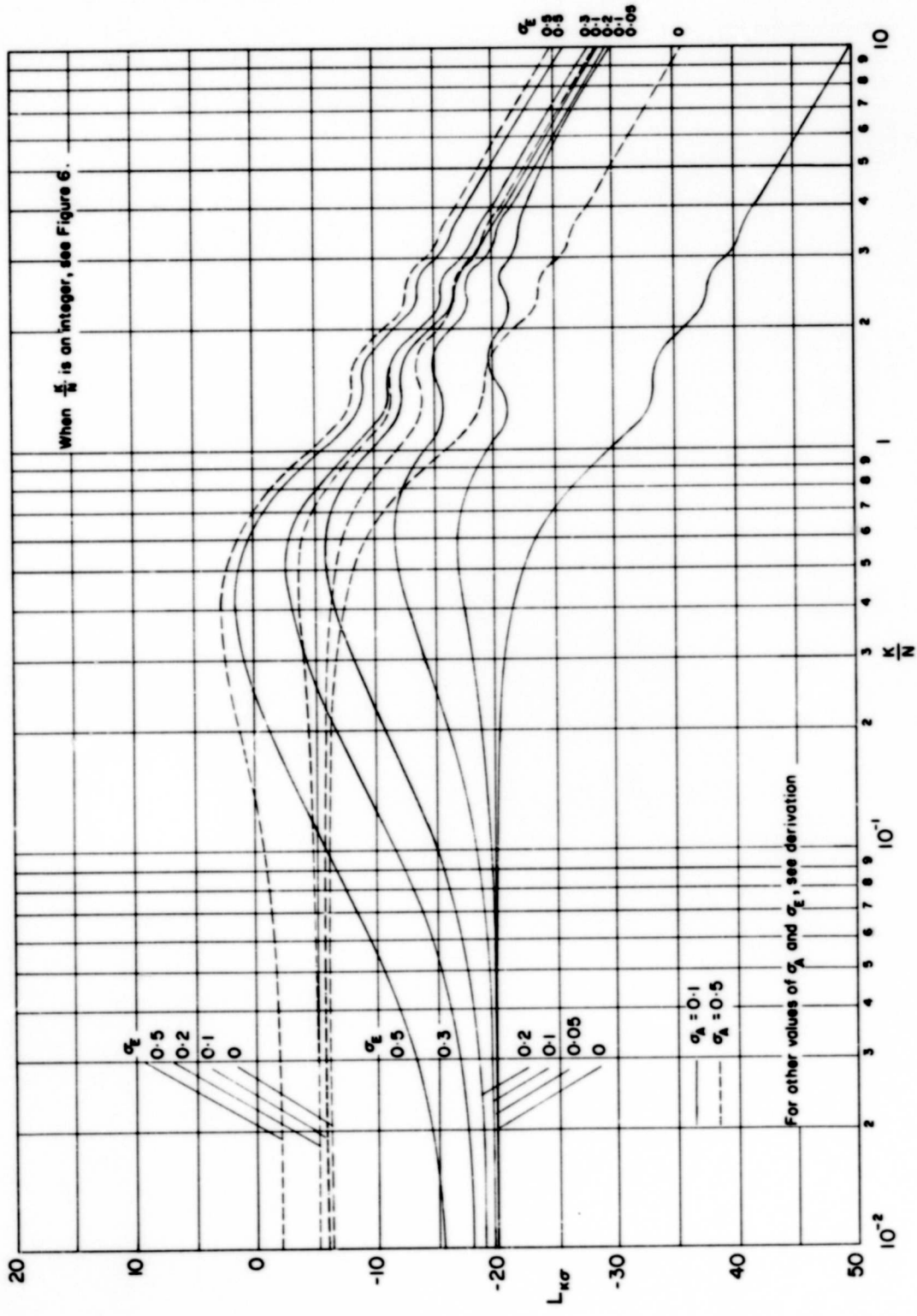


FIGURE 3.5 $L_{k\sigma}$ FOR $\frac{K}{N}$ NOT AN INTEGER

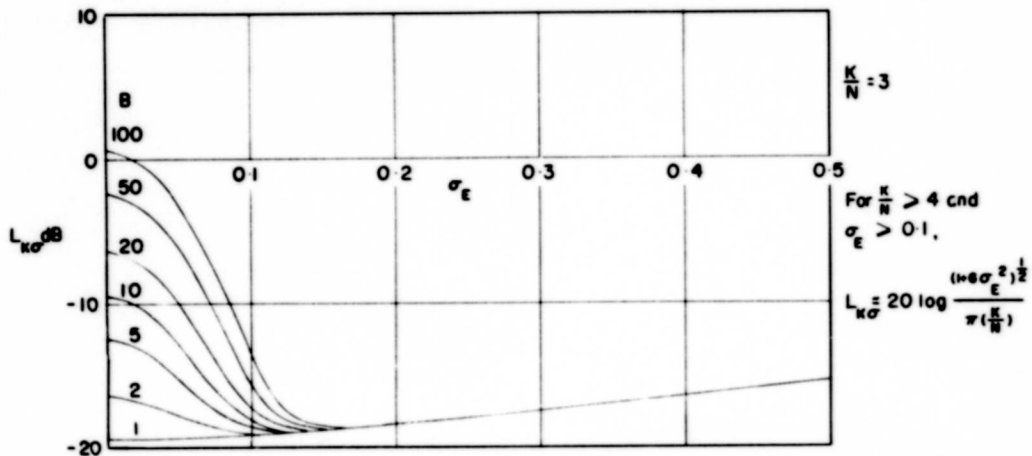
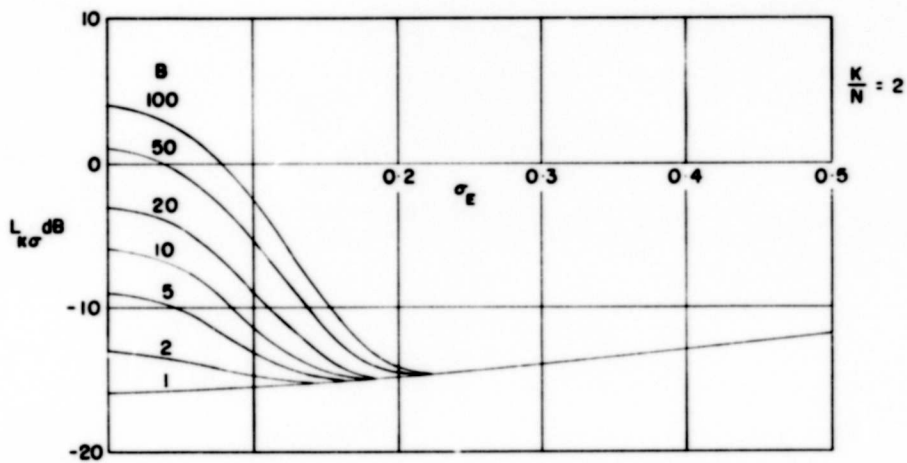
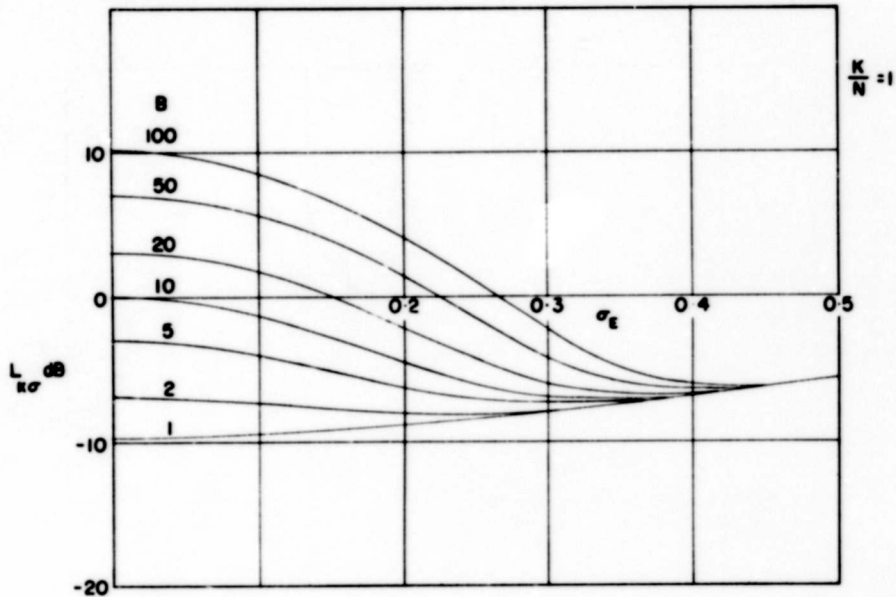


FIGURE 3.6 $L_{k\sigma}$ FOR INTEGER VALUES OF $\frac{K}{N}$

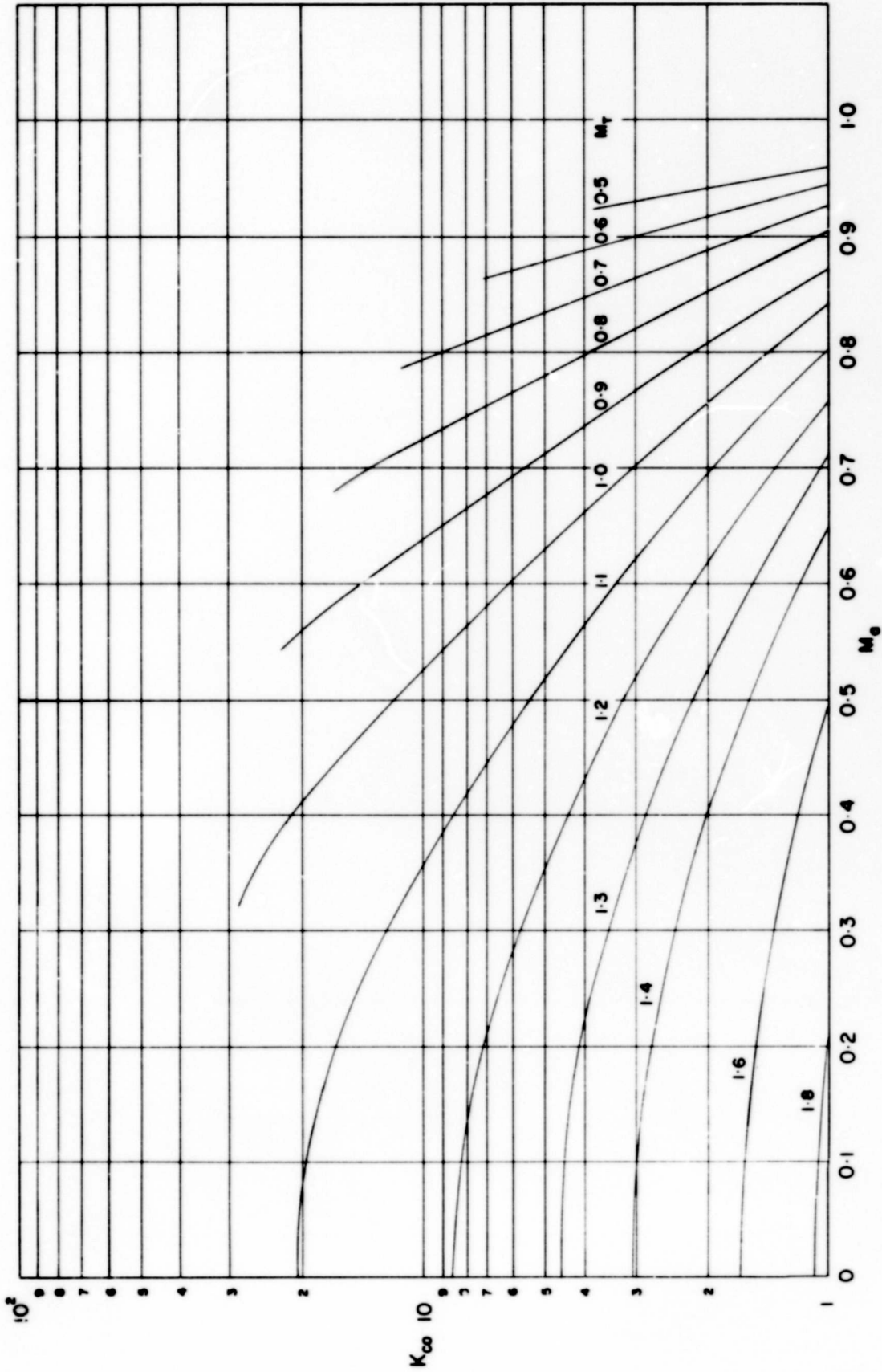


FIGURE 3.7 SHAFT ORDER NUMBER AT CUT OFF